General Disclaimer

One or more of the Following Statements may affect this Document

- This document has been reproduced from the best copy furnished by the organizational source. It is being released in the interest of making available as much information as possible.

- This document may contain data, which exceeds the sheet parameters. It was furnished in this condition by the organizational source and is the best copy available.

- This document may contain tone-on-tone or color graphs, charts and/or pictures, which have been reproduced in black and white.

- This document is paginated as submitted by the original source.

- Portions of this document are not fully legible due to the historical nature of some of the material. However, it is the best reproduction available from the original submission.

Produced by the NASA Center for Aerospace Information (CASI)

General Disclaimer

One or more of the Following Statements may affect this Document

- This document has been reproduced from the best copy furnished by the organizational source. It is being released in the interest of making available as much information as possible.

- This document may contain data, which exceeds the sheet parameters. It was furnished in this condition by the organizational source and is the best copy available.

- This document may contain tone-on-tone or color graphs, charts and/or pictures, which have been reproduced in black and white.

- This document is paginated as submitted by the original source.

- Portions of this document are not fully legible due to the historical nature of some of the material. However, it is the best reproduction available from the original submission.

Produced by the NASA Center for Aerospace Information (CASI)

Quarterly Report No. 2

REDUCED GRAVITY BATTERY TEST PROGRAM

Research and Development Center
General Electric Company
Schenectady, New York

Contract Number: 952121

October 1968

Prepared for:

Jet Propulsion Laboratory
California Institute of Technology
Pasadena, California 91109



N 69-10121
(ACCESSION NUMBER)
64
(PAGES)
CR-97471
(NASA CR OR TMX OR AD NUMBER)
(THRU)
1
(CODE)
03
(CATEGORY)
FACILITY FORM 602

S-68-1140

Quarterly Report No. 2

REDUCED GRAVITY BATTERY TEST PROGRAM

Research and Development Center
General Electric Company
Schenectady, New York

Contract Number: 952121

October 1968

This work was performed for the Jet Propulsion Laboratory, California Institute of Technology, as sponsored by the National Aeronautics and Space Administration under Contract NAS 7-100

This report contains information prepared by the General Electric Company under JPL subcontract. Its content is not necessarily endorsed by the Jet Propulsion Laboratory, California Institute of Technology, or the National Aeronautics and Space Administration.

FOREWORD

This report was prepared by the General Electric Company, Schenectady, New York, on J.P.L. Contract Number 952121. This contract is a subcontract under NASA Contract NAS 7-100, Task Order No. RD-26. This contract is administered by the Jet Propulsion Laboratory, California Institute of Technology, Pasadena, California. Mr. G. L. Juvinall is the designated JPL Technical Representative for the Laboratory.

The work presented in this Quarterly Report was accomplished between May 21, 1968 and August 20, 1968. The work was performed by the Research and Development Center of the General Electric Company.

Principal contributors were: A. J. Yerman, Technical Director; Dr. W. J. van der Grinten, Senior Chemical Physicist; J. M. Holeman, Engineer--Optic Systems; S. C. Richardson, Engineer--Measurements and Instrumentation; M. D. Ketchum, Engineer--Electronic Systems; and E. Siwek, Specialist--Battery Technology.

ABSTRACT

This is the second quarterly report of JPL Contract No. 952121 with the General Electric Company Research and Development Center covering the design, construction and testing of a breadboard model of test equipment capable of investigating the behavior of secondary Ag-Zn batteries in the zero-g environment of an earth orbit. Three types of test are to be performed automatically in sequence by the equipment.

This report covers the basic experimental work carried out to define the test procedure and equipment requirements of one of these tests which involves the photographic observation of gas bubble formation and distribution on the electrodes of a specially designed silver-zinc secondary battery during charge and discharge cycles. The cell and its peripheral equipment are described, and results are presented covering the partial discharge capacity of a porous zinc electrode as a function of the gas bubble coverage and current density.

Also included are experimental results pertinent to the other two tests which supplement and refine the information reported in the first quarterly report. These results include: (1) Test results showing the relationship between limiting current density and discharge capacity of smooth zinc electrodes oriented horizontally and vertically in a normal gravity environment. (2) The behavior of a Yardney type HR5-DC7 silver-zinc battery during a cyclic charge-discharge test at 65% of rated capacity conducted to destroy the battery.

TABLE OF CONTENTS

Title	Page Number
SECTION I -- INTRODUCTION	1
SECTION II -- TECHNICAL DISCUSSION	4
1.0 Task 1 -- Polarization of a Smooth Zinc Anode	4
1.1 Introduction	4
1.2 Test Procedures	5
1.2.1 Optimum Ramp Slope R_s	5
1.2.2 Current Ramp Circuitry	5
1.2.3 Differential Temperature Measurement	7
1.3 Test Results	9
1.3.1 Cell Measurements	9
1.3.2 Zinc Analysis	14
1.4 Discussion of Test Results	15
1.5 Conclusions and Recommendations	15
2.0 Task 2 -- Performance Dependence of Battery Electrodes on Trapped Gas	17
2.1 Introduction	17
2.1.1 Problem Areas	17
2.1.2 Exploratory Experimentation	18
2.2 Test Cell Construction and Operation	23
2.2.1 Cell Construction	23
2.2.2 Gas Bubble Collection and Removal	30
2.2.3 Activation	33
2.2.4 Optical Detection of Trapped Gas, Illumination and Photography	33
2.3 Preliminary Results	37
2.4 Conclusions and Recommendations	38
3.0 Task 3 - Testing of Commercial Secondary Silver-Zinc Cells	39
3.1 Introduction	39
3.2 Test Results	41
3.3 Discussion of Test Results and Recommendations	43
SECTION III -- CONCLUSIONS	50
SECTION IV -- RECOMMENDATIONS	53
SECTION V -- NEW TECHNOLOGY	55

LIST OF FIGURES

Figure No.	Title	Page Number
1-1	Log LCD and Log C_d Plotted as a Function of Log R_s	6
1-2	Task 1 Ramp Generator and Control Circuit	8
1-3	Cross-Sectional View of the JPL-Arcand Silver-Zinc Cell with Thermocouples	10
1-4	Typical LCD Recording of Task-1 Run	11
2-1	Exploratory Test Cell (Zn)	19
2-2	Zinc Discharge With and Without Gas Coverage	22
2-3	Complete Test Cell Assembly	24
2-4	Exploded View of Test Cell Assembly	25
2-5	Details of Test Electrode and Counter Electrode in Task 2 Test Cell	27
2-6	Top View of Cell Flange With 3 Electrodes and KOH Input Tube	28
2-7	Exploded View of Electrode Arrangement	29
2-8	Auxiliary Equipment for Gas/Liquid Separation, Evacuation, Backfill and Activation	31
2-9	Photomicrograph of Zinc Test Electrode	35
2-10	Camera and Test Cell Arrangement for Task 2	36
3-1	Cell Voltage, Cell 5, Test 1	44

LIST OF FIGURES

Figure No	Title	Page Number
3-2	Cell Voltage, Cell 5, Test 2	45
3-3	Cell Voltage, Cell 5, Test 3	46
3-4	Cell Voltage, Cell 5, Test 4	47
3-5	Cell Voltage, Cell 5, Test 5	48

LIST OF TABLES

Table No.	Title	Page Number
1-1	Reduced Gravity Battery Test, Individual Points	12
1-2	Reduced Gravity Battery Test, Average Values	13
3-1	Preliminary Task 3 Test Sequence	40

SECTION I - INTRODUCTION

This is the second quarterly report issued as a part of the requirements of Contract Number 952121 between California Institute of Technology, Jet Propulsion Laboratory and the Research and Development Center of the General Electric Company.

Under this contract which started February 21, 1968, the Research and Development Center has taken on the responsibility of designing, fabricating, and testing a breadboard unit of a test system which is to be capable of investigating the behavior of silver-zinc battery cells during flight in a low or zero-g environment. The breadboard unit is to be capable of conducting three separate tests which have been assigned task numbers and are defined as follows;

Task 1 - To measure the limiting current density of a smooth, pure zinc anode in the region of 0 to 1g, in an experiment designed to provide maximum correlation with data previously obtained by JPL over a 1-20g range.

Task 2 - To investigate the performance of battery electrodes in a special silver-zinc research cell as a function of bubble formation on the electrode surfaces.

Task 3 - To measure the electrical capacity of a commercial secondary silver-zinc cell as a function of charge-discharge cycling in a 0 to 1 g environment as well as the limiting current capability (polarization curve).

During the second quarter of this contract, effort has been concentrated on the detailed delineation of test procedures and the design of the test system for implementing them in the breadboard model. In order to select the

best procedures, it has been necessary to perform a considerable amount of laboratory testing of sample cells to establish characteristics and/or design adequacy.

The results of these tests comprise this report and consist of the items described in the following paragraphs.

Section 1.0 of the Technical Discussion presents the results obtained in an experiment designed to measure the Limiting Current Density of Task 1 cells as a function of electrode orientation in a normal gravity field, and the discharge capacity; the latter being controlled by varying the slope of the discharge current ramp employed to polarize the cell. This information was necessary to evaluate the adequacy of the current ramp approach by permitting a comparison of results with previous measurements made by JPL. Somewhat different methods were used in those tests which would have been very difficult to implement in an automatic test.

Section 2.0 covers the results obtained with special designs of silver-zinc batteries which permit observation of bubble formation on electrodes during charge and discharge. These cells have been developed to meet the requirements of Task 2 measurements. Data are presented which form the basis for the test procedure to be employed in the Task 2 tests.

Early in this program, the Yardney HR5-DC7 Battery was selected as representative of commercially available silver-zinc secondary cells, and therefore a suitable subject for Task 3 tests. Some initial tests were reported on last quarter which were designed to determine loss of capacity during cyclic charge-discharge at 35% of rated capacity. Further tests of this type are reported on here which differ in that they have been performed automatically using micro-circuit logic, and a depth of discharge of 65% of rated capacity. These tests, reported on in Section 3.0, had the twofold

purpose of providing an evaluation of proposed test circuits, and also of providing additional insight into the behavior of a typical battery during a cyclic test to destruction.

While considerable effort was devoted during this quarter to the detailed design of equipment to implement proposed test procedures, the results of that effort were presented in R & DC Report S-68-1118 titled "Test Plan and Test Procedures for Reduced Gravity Battery Test Program" issued July 1968, and hence are not included in this report.

SECTION II - TECHNICAL DISCUSSION

1.0 Task 1 - Polarization of a Smooth Zinc Anode

1.1 Introduction

It is the objective of this task to measure the limiting current density (LCD) of the smooth pure zinc anode of a silver-zinc cell with the zinc electrode positioned in the vertical and horizontal directions. The experiment shall be designed in such a way as to provide maximum correlation with data previously obtained by JPL.

As explained in Quarterly Report No. 1 (Section 1.1) the LCD-determining transport processes are gravity dependent, if the zinc electrode is placed in the vertical position. In the horizontal zinc position, on the other hand, such processes are not normally gravity dependent so that the horizontally oriented zinc electrode at the bottom and at 1-g can be looked upon, at least qualitatively, as a "simulation" of the o-g environment.

During the first quarter a cell was designed for maximum correlation and its construction, testing procedure and preliminary performance was described and discussed in the first quarterly report. In the interest of less complex automated programming it was decided to use linear current ramps (with a slope R_s), starting at zero current, for determining the limiting current density of the zinc-electrode. This constitutes a deviation from the earlier practice of using step-functions. Cell performance and exploratory results obtained on vertically oriented zinc electrodes with current ramps were encouraging. However, circuit deficiencies and excessive discharge capacities ($C_d = \frac{LCD^2}{2R_s}$) were encountered particularly with horizontal testing, which needed correction. These and other minor difficulties have been corrected during the present reporting period, using the same cell and component preparation described earlier.

1.2 Test Procedures

1.2.1 Optimum Ramp Slope R_s

The desire for maintaining a reasonably well balanced depth of discharge C_d in order to maintain an equivalent degree of etching of the polished zinc-electrode and similar specific gravity changes of the electrolyte, regardless of orientation, has already been discussed in the previous report. This, in turn, led to the desirability of using different ramp slopes for the different electrode orientations with correspondingly different LCD values. It is useful to discuss the reasoning for this with the help of a semi-quantitative version of Figure 1-3 of Quarterly Report No. 1 given here as Figure 1-1. Both figures illustrate log C_d and log LCD as a function of log R_s for the vertical and horizontal zinc electrode orientations.

Starting with a shallow R_s (6.9 ma/min.) in the horizontal position (subscript zero) we find LCD_o and C_{d_o} to be both "low" (see situation I). Shifting to the vertical situation II we now find a higher LCD_1 value as expected but, unfortunately, C_{d_1}, of this measurement, because of its LCD^2 - proportionality, is also much higher. Moving now to situation III with the "steep" R_s of 62 ma/min. we can now attempt to re-establish again the original standard C_d of I without impairing LCD, as desired. In this particular example the C_d - correction turned out to be somewhat too large.

The degree of matching the C_d-values of situations I and III will depend on the R_s - values selected, among other things. The proper match may require some trial and error approach.

1.2.2 Current Ramp Circuitry

The ramp generator for the Task 1 bench top tests was outlined in both Quarterly Report #1 and the Test Plan. A detailed schematic diagram is shown

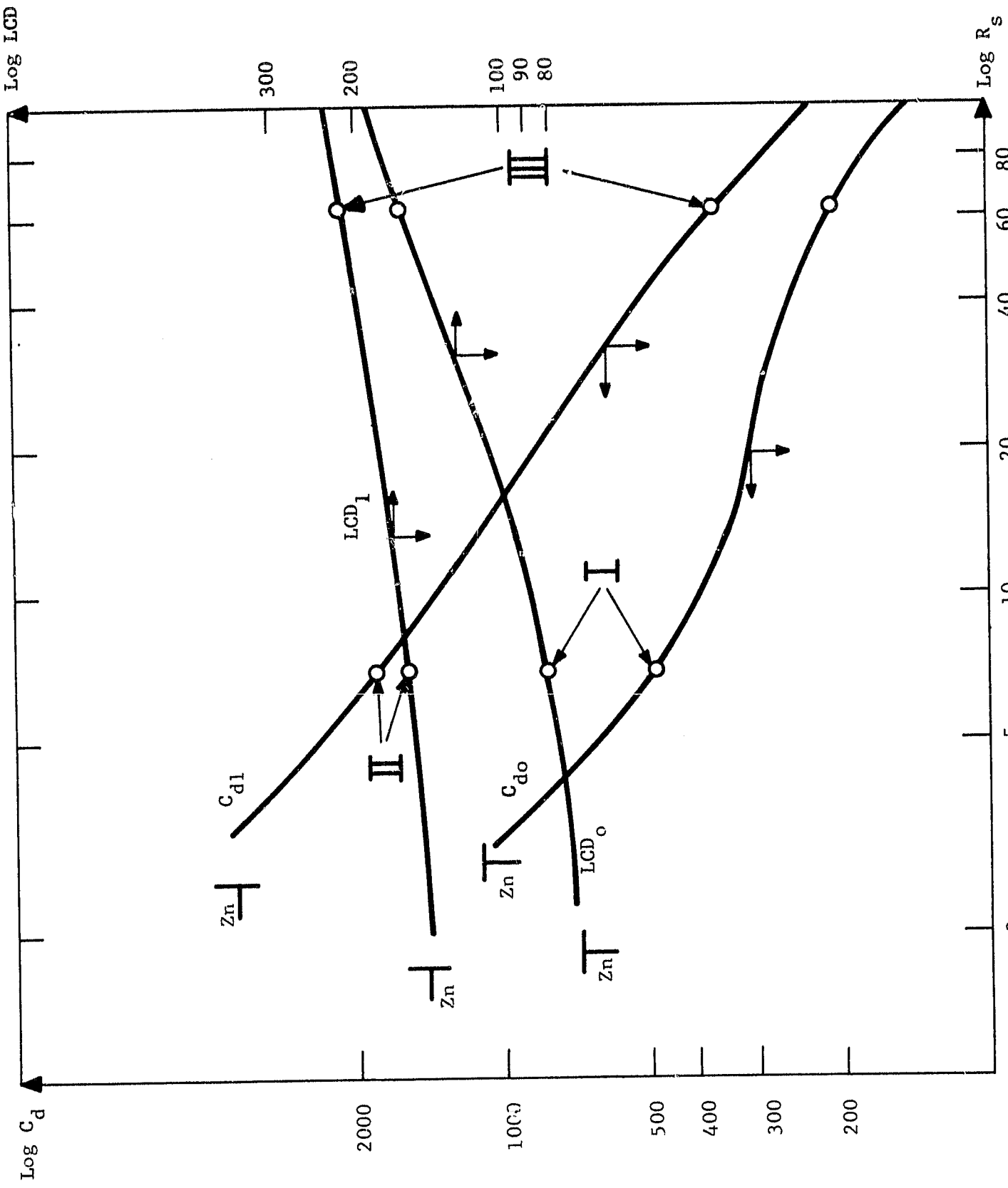


Figure 1-1 Log LCD and Log C_d Plotted as a Function of Log R_s

in Figure 1-2. The ramp generator and discharge current control circuit provide switch selected slopes of approximately 7 and 60 ma/min.

The ramp generator is a Bell and Howell type 20-008-01 operational amplifier that is used as an integrator. The integrator is formed by the combination of the 10μf capacitor and the high value input resistance. Two input resistances are switch selected to provide the two ramp rates. The output of the ramp generator is attenuated and fed to the cell current control circuit. The ramp is linear to better than 1% from the best straight line.

The discharge current control circuit consists of a Fairchild 709 operational amplifier, a 2N3054 control transistor and a current measuring resistor. The voltage from the ramp generator on the positive input of the 709 turns on the 2N3054. Cell current flowing through the .5Ω (or .25Ω) resistances produces a voltage drop which exactly counteracts the input voltage. The effect is a current control circuit where the cell discharge current follows the input voltage. Since the input voltage is a voltage ramp, the discharge current is a current ramp. A switch selected resistance in the current measuring circuit is provided to keep the "X-Y" recorder on scale for both ramp rates.

The voltage drop across the current measuring resistance and the saturation voltage of the control transistor combine to produce a minimum cell voltage where the control circuit can function. This minimum voltage is on the order of 0.2 to 0.3 volts. This is low enough to produce the type of cell measurement desired.

1.2.3 Differential Temperature Measurement

The conditions prevailing in a zero gravity environment can be simulated effectively only if the discharging cell in the horizontal position remains free of convection currents in the electrolyte. Any heating of the zinc

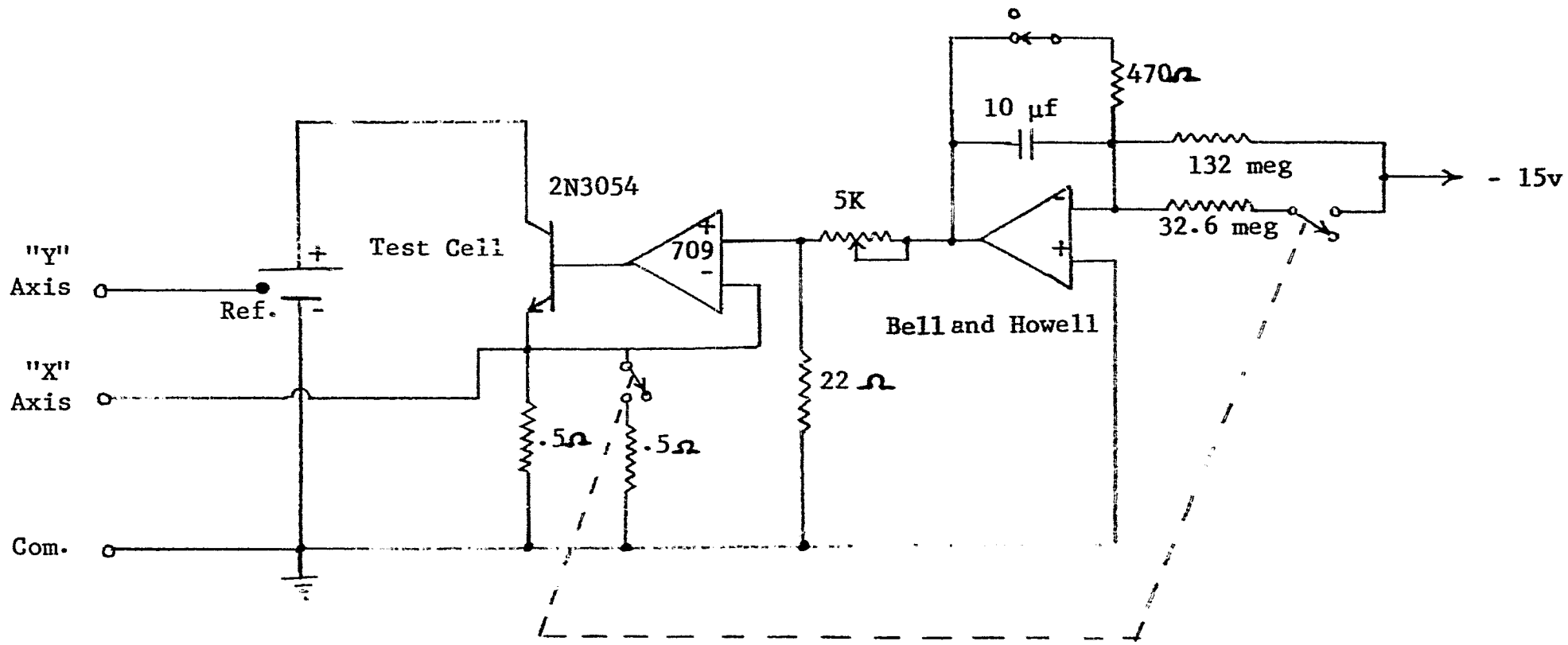


Figure 1-2

Task 1 Ramp Generator and Control Circuit

electrode during discharge could produce a temperature gradient inside the electrolyte layer, leading to such a convective disturbance. Since the magnitude and distribution of heat evolution during ar LCD - measurement and its resultant temperature pattern is not easily calculable, it was decided to determine any existing temperature differentials (ΔT) inside the electrolyte experimentally.

Figure 1-3 illustrates the cell modification selected for this. Two open ended glass capillaries are inserted and sealed into the cell body as shown: one parallel and close to the zinc electrode, the other in the vicinity of the silver electrode. A differential Chromel-Alumel thermocouple was mounted inside and the ΔT was monitored during a run with a microvoltmeter. As indicated in the next section maximum ΔT values were less than $1^{\circ}C$ even for the highest current and deepest discharge levels.

1.3 Test Results

1.3.1 Cell Measurements

Using the improved current ramp slope generator and the standard cell previously described, 12 new LCD - measurements of standard zinc electrodes were made at ramp slopes of 6.9 and 62 ma/min. with both vertical and horizontal zinc electrode orientations. During a run the zinc to reference electrode voltage was recorded on a X-Y recorder, shown in Figure 1-4, as a function of cell current. Since this current is a linear function of time, the X-axis represents elapsed time as well as current level. Table 1-1 lists the individual measurements.

Table 1-2 lists the average values of these 12 tests. Each data point given represents an average of three runs. These data points were also used for the preparation of Figure 1-1. Consistency of data has benefited greatly

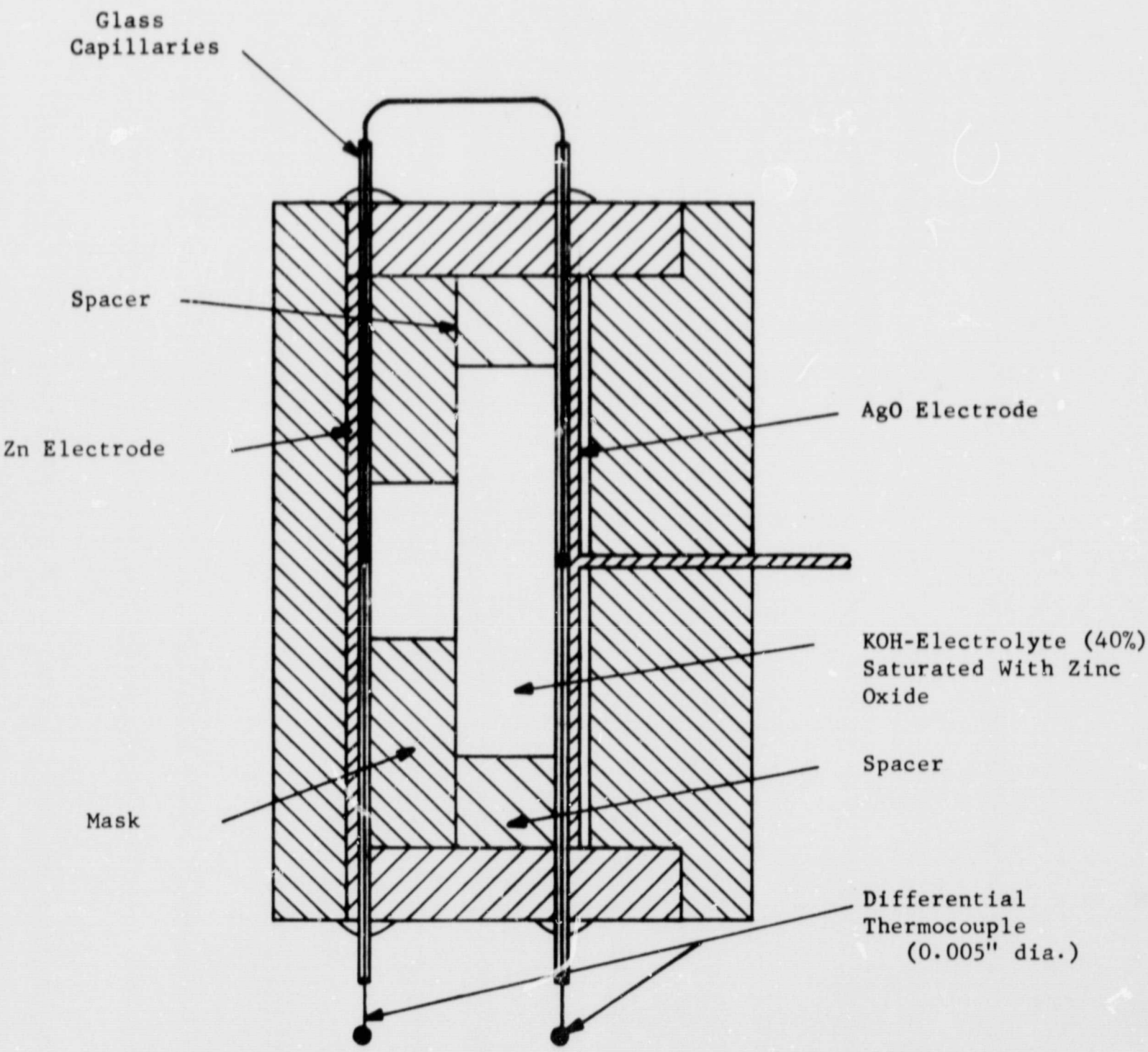


Figure 1-3 Cross-Sectional View of the JPL-Arcand Silver-Zinc Cell with Thermocouples

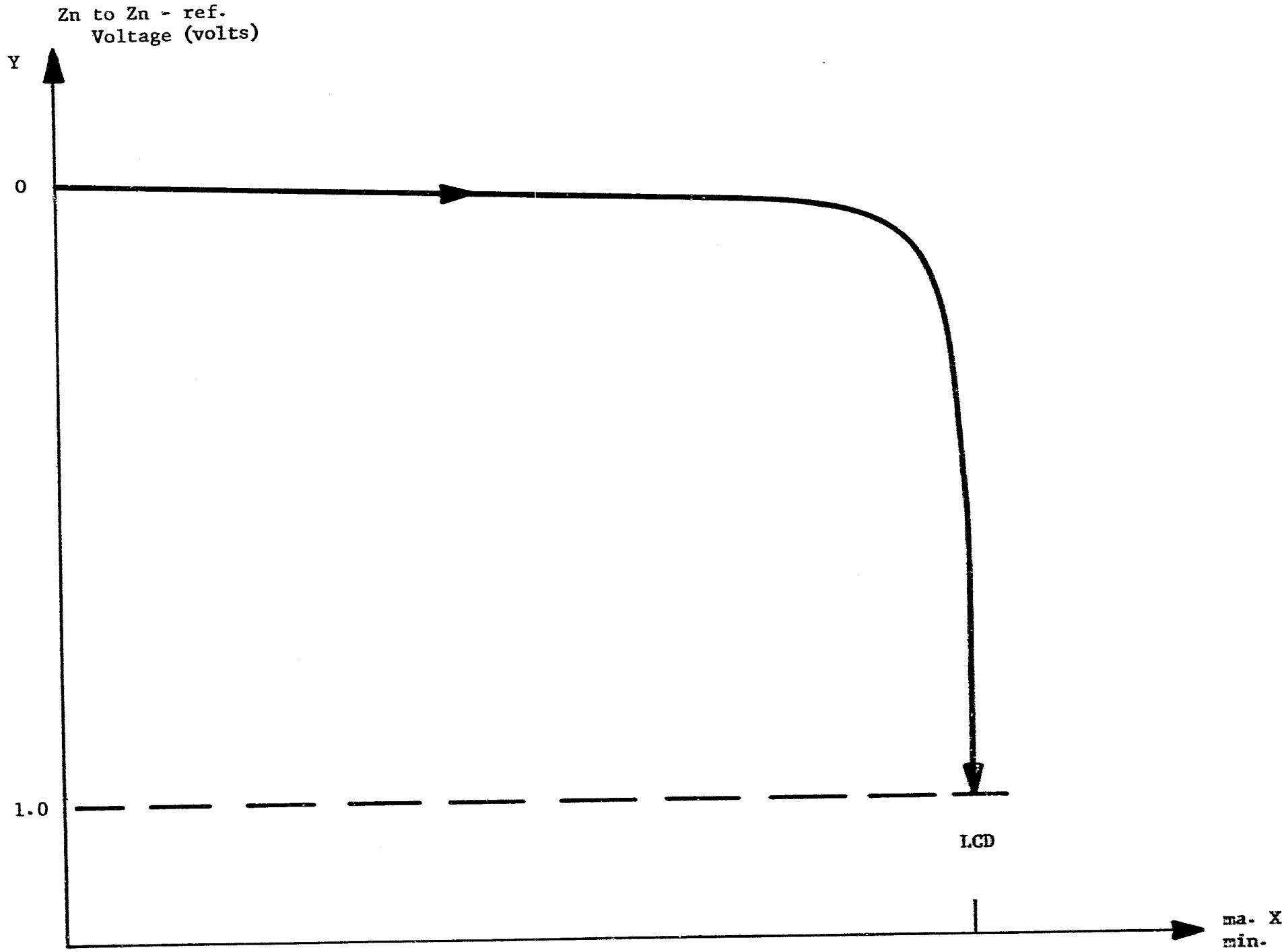


Figure 1-4 Typical LCD Recording of Task-1 Run

Table 1-1

REDUCED GRAVITY BATTERY TEST, INDIVIDUAL POINTS

Test No.	Orientation	Ramp Slope R_s (ma/min.)	Limiting Current Density LCD (ma)	Time to Passivation (min.)	Capacity Discharged C_d (ma.min.)
1	Vertical	62	208.7	3.37	351
7	Vertical	62	215.4	3.47	374
11	Vertical	62	216.5	3.49	378
3	Vertical	6.9	148.0	21.4	1729
5	Vertical	6.9	156.8	22.6	1782
9	Vertical	6.9	166.7	24.1	2004
4	Horizontal	62	157.7	2.54	201
6	Horizontal	62	160.8	2.59	208
10	Horizontal	62	165.4	2.67	221
2	Horizontal	6.9	86.3	12.4	537
8	Horizontal	6.9	75.9	11.0	415
12	Horizontal	6.9	83.3	12.0	501

TABLE 1-2

REDUCED GRAVITY BATTERY TEST, AVERAGE VALUES

Orientation	Ramp Slope R_s (ma/min)	Situation	Limiting Current Density LCD (ma)	Time to Passivation (min)	Capacity Discharged C_d (ma-min)
Horizontal	6.9	I	82	11.8	484
Vertical	6.9	II	157	22.7	1838
Vertical	62	III	214	3.4	368
Horizontal	62	-	161	2.6	210

from the use of the new current ramp equipment.

After these 12 tests the cell was modified, to permit the differential thermocouple measurements discussed earlier to be made. Even under extreme conditions (e.g. 1838 ma.min. discharge) this ΔT was found to be less than one degree C.

1.3.2 Zinc Analysis

After the completion of this part of the program one 10 gram sample of our zinc supply* was analyzed, using a Perkin-Elmer Model 303 Atomic Absorption Spectrophotometer. The following impurity levels expressed in weight percent were found:

copper	0.006
lead	0.002
cadmium	0.002
iron	0.001
Total	0.011%

Other types of zinc were analyzed the same way and were found to exhibit lower impurity levels. This includes Battery Grade zinc obtained from the New Jersey Zinc Company.

Conceivably such impurity levels may have a small effect on LCD - values. However, since the JPL-Arcand tests were performed, using the same type of zinc (although not necessarily the same lot), the maximum correlation requirement stated earlier may not be seriously impaired by this finding. It is unfortunate, nevertheless, that this discovery was not made during the earlier part of this program.

---

*obtained from the Electronic Space Products, Inc. and indicated to be 99.999% pure.

1.4 Discussion of Test Results

Results can be summarized as follows:

a. Comparing situations I and II the LCD - ratio

$$LCD_1/LCD_0 = \frac{157}{82} = 1.91$$

but unfortunately C_d's are poorly matched (484 and 1838 ma.min.).

b. Comparing situations I and III the LCD - ratio

$$LCD_1/LCD_0 = \frac{214}{82} = 2.6$$

and the C_d match is greatly improved (484 and 368).

c. Still better matching could be expected if the two ramp slopes were somewhat closer together (e.g. 7 and 50 ma/min.).

d. Our situation II LCD's match the JPL-Arcand data very well.

e. Electrolyte temperature gradients in the horizontal position are very small.

1.5 Conclusions and Recommendations

A critical examination of Table 1-1 reveals the excellent reproducibility of the new LCD - measurements. Since both test plan and flight units are designed for a Task 1 test series of six cells, adequate reliability and accuracy is to be expected.

Minor adjustments of ramp slopes may be necessary, if near perfect discharge capacity matching for vertical and horizontal measurements is desired. It is therefore advisable to include some adjustability of the ramp slope in the breadboard model, to permit JPL to make further refinements, if desired.

From the small temperature differences measured with the electrode horizontally positioned, it can be concluded that thermal convection is a negligible factor in determining electrode performance. This follows from a consideration of the thermally induced changes in electrolyte density, contrasted to density changes due to dissolution of zincate ($K_2Zn(OH)_4$) in the electrolyte. Eisenberg* has reported an increase in density from 1.294 to 1.411 gm/cm^3 as a 30% KOH electrolyte solution becomes saturated with zincate due to the discharge of a zinc electrode. This increase in density of approximately 9% compares with a decrease in density of only 0.04% $^{o}C^{-1}$ for a 40% KOH solution. Thus it can be concluded that any tendency toward thermal convection due to a $1^{o}C$ gradient would be largely masked by the stabilizing effect of the zincate layer.

Thus, in view of the measured homogeneity of the temperature distribution at both high and low rates, the horizontal electrode configuration can be expected to simulate the o-g condition adequately.

The results obtained are fully compliant with the stated objectives. The initiation of the next phase, i.e. the execution of the test plan, is therefore recommended.

---

* M. Eisenberg, H. F. Bauman, D. M. Brettner: "Gravity Field Effects on Zinc Anode Discharge in Alkaline Media," J. Electrochem. Soc., 108, 909, (1961).

2.0 Task 2 - Performance Dependence of Battery Electrodes on Trapped Gas

2.1 Introduction

It is the objective of this task to investigate the performance of silver-zinc battery electrodes as a function of the photographically recorded presence or absence of gas bubbles on the electrode surfaces. This study shall include measurements of the electrical capacity of a research cell during a cycle designed to induce bubble formation as well as a record of the physical behavior of the bubble and the gas-liquid phase distribution within the cell. It must be possible to perform this study in a 0-g environment.

The unusual features of this assignment have made it necessary to conduct a considerable amount of time-consuming preliminary research and development prior to the formulation of the test plan. Although such R&D has been conducted since March 1968, its progress was not reported on in the First Quarterly Progress Report. The following detailed account of this task will therefore cover all facets of the work performed since its inception.

2.1.1 Problem Areas

An analysis of the unusual features of this electrode study has resulted in the formulation of the following problem areas:

a. In order to be able to study the battery type silver and zinc electrodes in the presence and absence of gas bubbles, provisions must be made to add and remove such gas bubbles at will. Although the addition of gas to an electrode is readily achieved during overcharge, its removal from a high porosity electrode requires special attention.

b. The observation and recording of a distribution of gas bubbles inside the high porosity electrodes of a silver-zinc cell is not normally possible.

c. What type of electrical discharge stress will respond to the presence or absence of trapped gas?

d. How can such correlation be optimized and measured conveniently?

e. How can test cells suitable for items a thru d be adapted for use in outer space?

f. How can test cells suitable for items a thru e be adapted for automated testing.

Since conventional battery technology provides no ready-made answers to these questions, new methods for the solution of these problems had to be conceived and explored.

2.1.2 Exploratory Experimentation

Practical solutions to some of the above mentioned problems have been derived from experimentation with an exploratory test cell, a simplified version of which is illustrated in Figure 2-1. A small circular test electrode is mounted at the center of an open rectangular outer plexiglass tray, which also contains the electrolyte. A U-shaped stainless steel spring (not shown) presses a supported transparent membrane separator firmly against the upper surface elements of the test electrode. An inner funnel-shaped plexiglass tray, equipped with two submerged counter electrodes mounted sideways as shown, is positioned on top of the test electrode in a way which guarantees homogeneous ionic current distribution at the test electrode level and good visibility from above. A small zinc reference electrode is positioned in the immediate vicinity of the test electrode, to permit the measurement of realistic

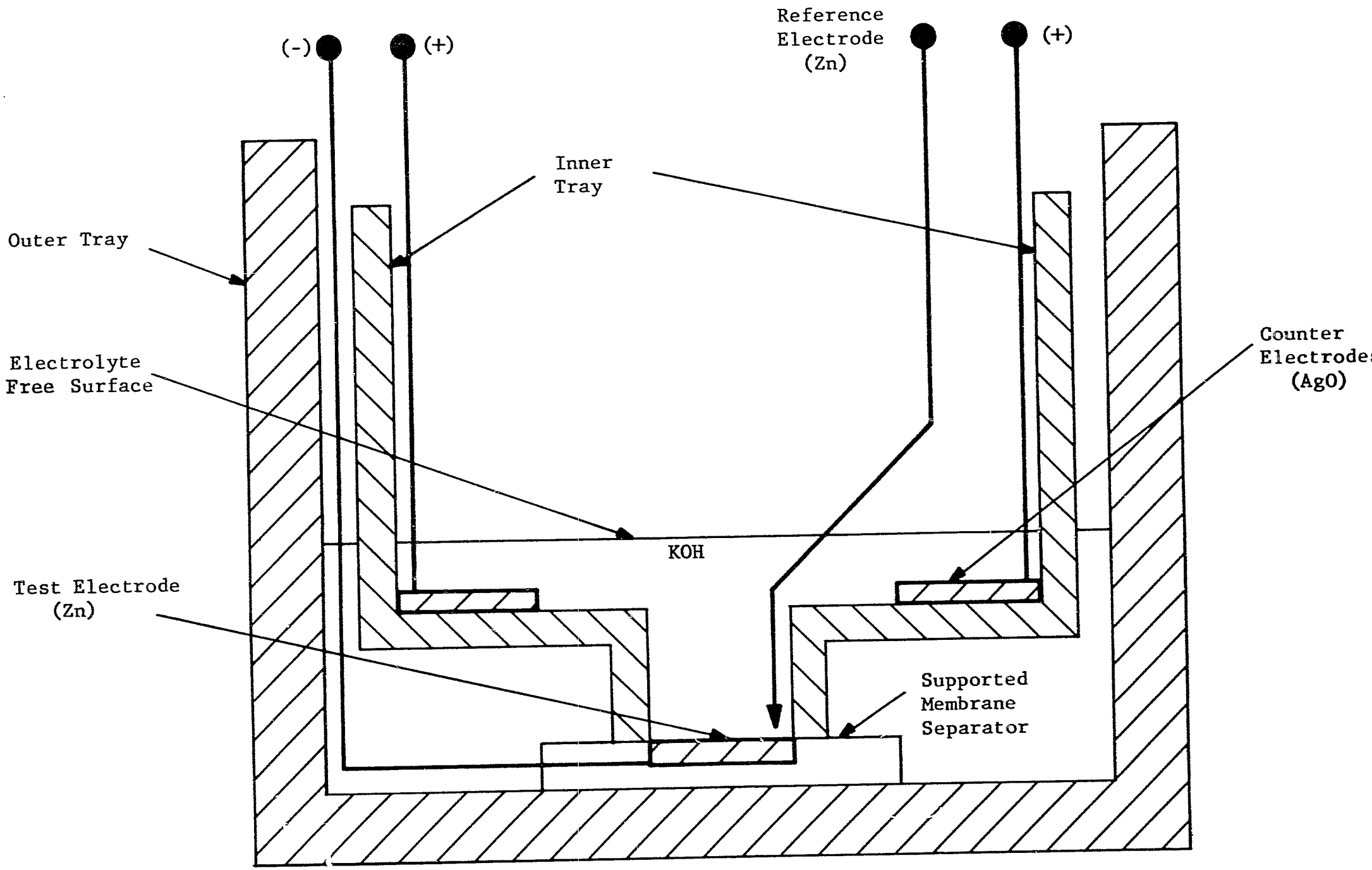


Figure 2-1 Exploratory Test Cell (Zn)

test electrode polarizations at high current densities. The test electrode is examined optically from above through the free surface of the KOH electrolyte by means of a low power binocular microscope.

The following observations were made:

1. Although the optical properties of the electrolyte, its surface and the membrane separator (cellophane) layer are quite adequate, the visibility of gas bubbles against the back-ground of high-porosity electrode material is marginal.

2. Such contrast can be greatly enhanced by taking advantage of the specular reflection of the narrow illuminator beam occuring at the lower membrane surface whenever a gas bubble touches the membrane. This transforms the non-reflective electrolyte-membrane interface locally into a reflective gas-membrane interface. The presence of such flattened-out, pancake-type gas bubbles is a common occurrence at any flat boundary of a high-porosity medium, regardless of orientation, particularly if the pore sizes are small.

3. Gas bubbles embedded within the bulk of the porous electrode cannot be seen.

4. Gas bubbles formed during overcharge (hydrogen on the zinc electrode or oxygen on the silver-oxide electrode) can easily be removed by placing the exploratory test cell inside a dessicator and by evacuating the dessicator once or twice. This reduces the specular reflection type gas coverage from a high value (i.e. 70-90%) to less than 10%.

5. Because of the large excess of zincate containing electrolyte present in these "optical" cells, the discharge capacity of the zinc test electrode changes with cycling. Therefore, the effect of bubble formation on capacity must be measured rapidly.

6. The effect of substantial gas coverage on the discharge capacity at low current densities is negligible.

7. The effect of substantial gas coverage on the discharge capacity at high current densities can be quite significant.

8. Comparing such effects for both zinc and silver electrode test cells, the deleterious effect of gas coverage on the capacity of the zinc test electrode was found to be greater.

In view of the constraints mentioned in items 5 and 6 the following testing procedure was found to be useful:

Step 1: Activate the evacuated cell, charge and overcharge the test electrode.

Step 2: Determine the partial discharge capacity D_1 of the fully charged and gas loaded test electrode at a high constant current density.

Step 3: Remove the trapped gas from this test electrode within a few minutes by means of cell evacuation and backfilling.

Step 4: Resume discharge at the same constant current density and determine the residual discharge capacity D_2 in the absence of trapped gas.

If trapped gas has no effect, one should find the ratio of D_2/D_1 to be essentially zero. As mentioned in item No. 6, this is the case at low current densities. On the other hand, for current densities in the 50-100 ma/cm^2 region, D_2/D_1 ratios in excess of 1.1 were obtained, using a 3/8" OD pellet of the Yardney HR-5 porous zinc-electrode material as a zinc test electrode.

Figure 2-2 illustrates the type of polarization characteristic obtained on zinc. The Zn/Zn (ref) voltage is plotted as a function of time. At a constant discharge current of 40 ma (56 ma/cm^2) the hydrogen loaded zinc test electrode can be seen to polarize excessively after 24 minutes.

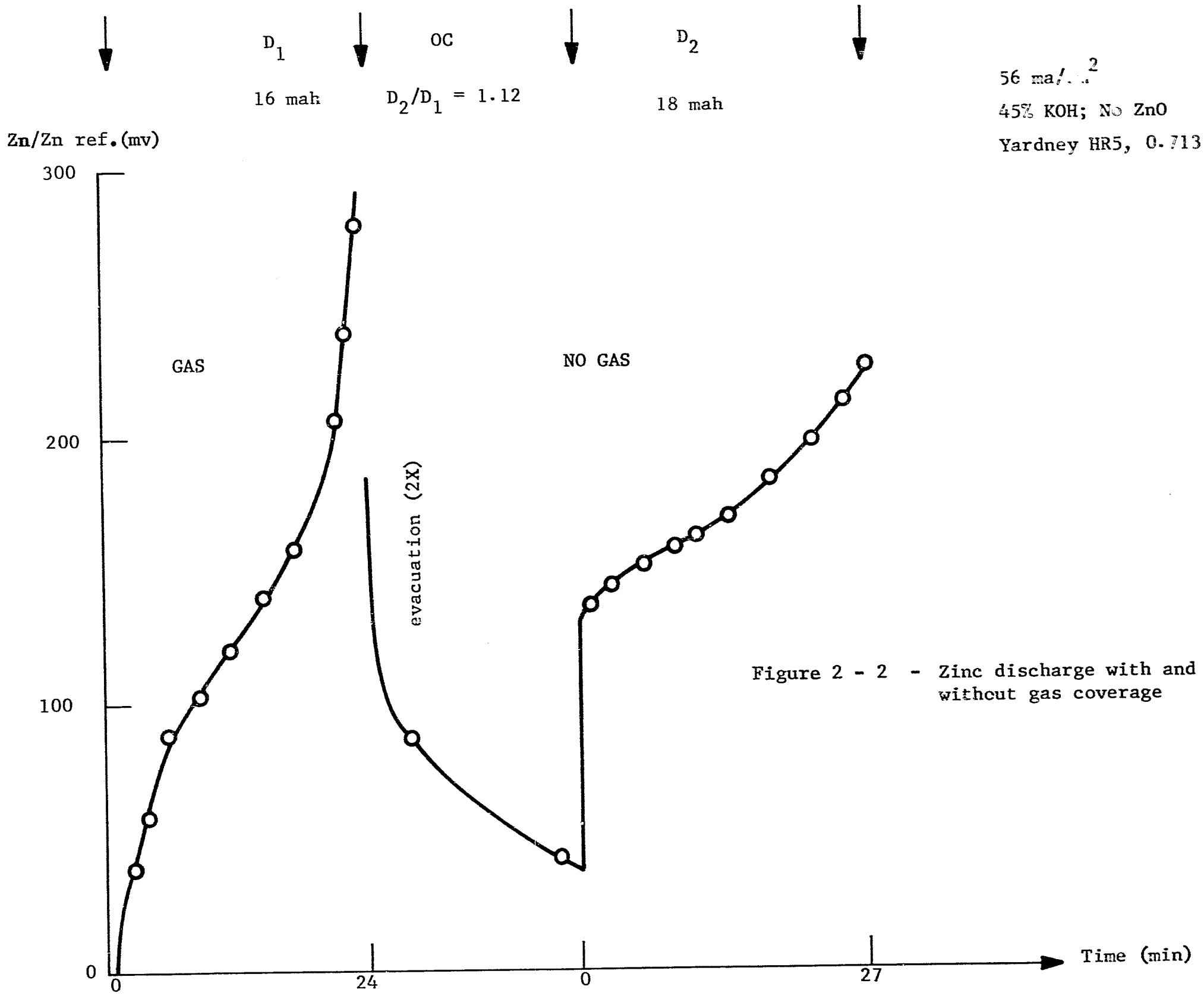


Figure 2 - 2 - Zinc discharge with and without gas coverage

This corresponds to a discharge capacity D_1 of 16 ma-hrs. During the following open circuit period the exploratory test cell was evacuated twice. Discharge D_2 for minimum gas coverage at the same current density was initiated after that and maintained for an additional 27 minutes at a comparable polarization level. This corresponds to an additional 18 ma-hrs of discharge capacity, which was not available during maximum gas coverage. For a Yardney HR-5 silver electrode pellet, tested at 100 ma/cm^2, a D_2/D_1 ratio of 0.47 was measured.

2.2 Test Cell Construction and Operation

The exploratory phase of this task previously described, has certainly provided valuable solutions to some of the basic problems stated earlier. Nevertheless, the test cell in this form is not suitable for incorporation into the test plan because its proper functioning is greatly dependent on the presence of gravity and its adaption to automated testing procedures would be complicated. Consequently a new test cell model has been conceived and constructed which is fully compatible with 0-g and with automation. The basic difference between the old and the new model is the use of a closed system circulating electrolyte, to prevent free gas bubbles from interfering with the optics and the use of a special "strainer" to help separate and remove gas bubbles from the electrolyte in a 0-g environment. Two physically and electrically separate cell systems are to be built, one for the zinc test electrode and one for the silver test electrode, with only the photographic recording apparatus and the vacuum manifold common to both. Other minor differences will become apparent from the description which follows.

2.2.1 Cell Construction

Figures 2-3 and 2-4 show the complete assembly and the exploded view of one of the test cells. Flange No. 3 contains the three electrodes, i.e. the

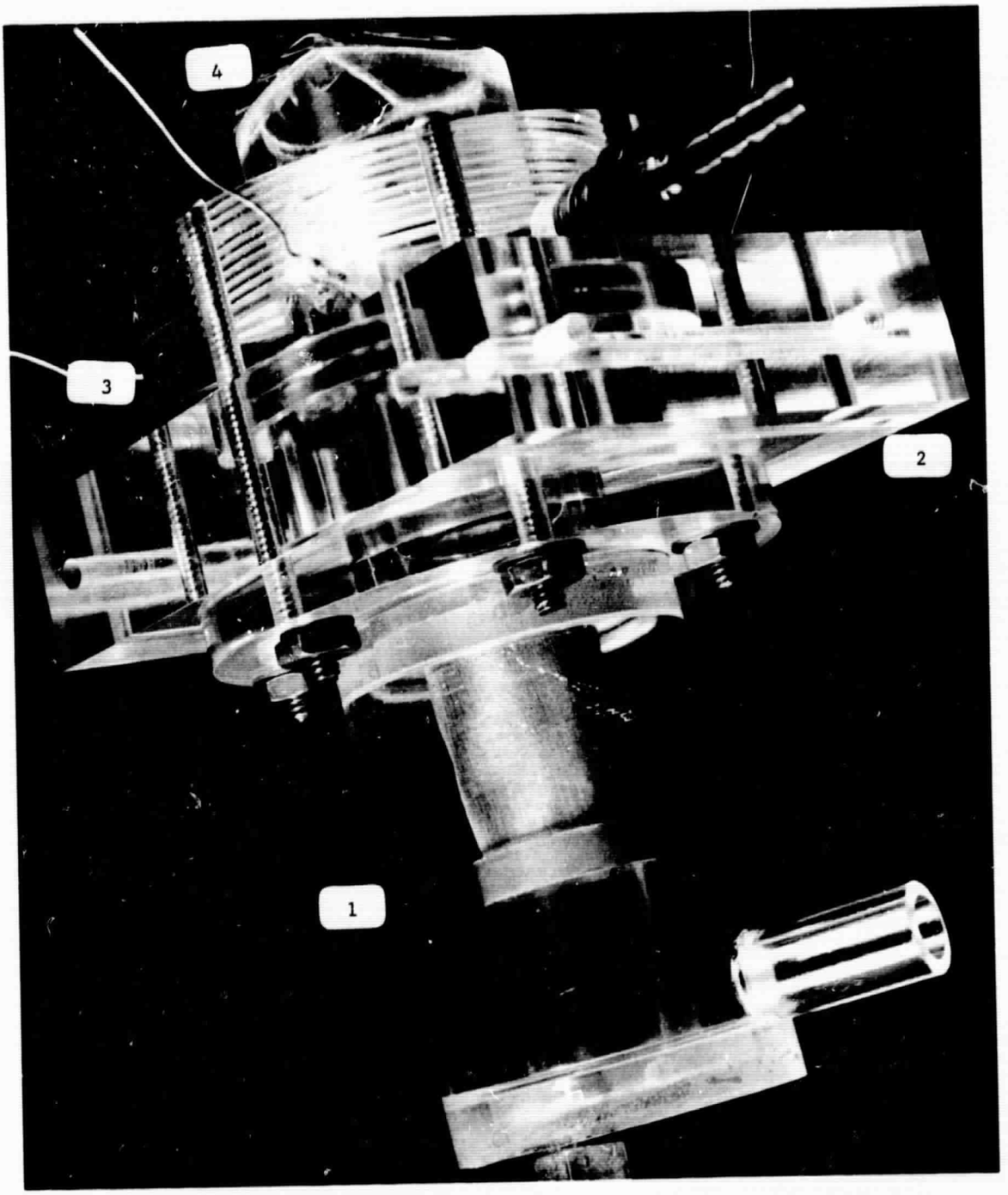


Figure 2-3. Complete Test Cell Assembly

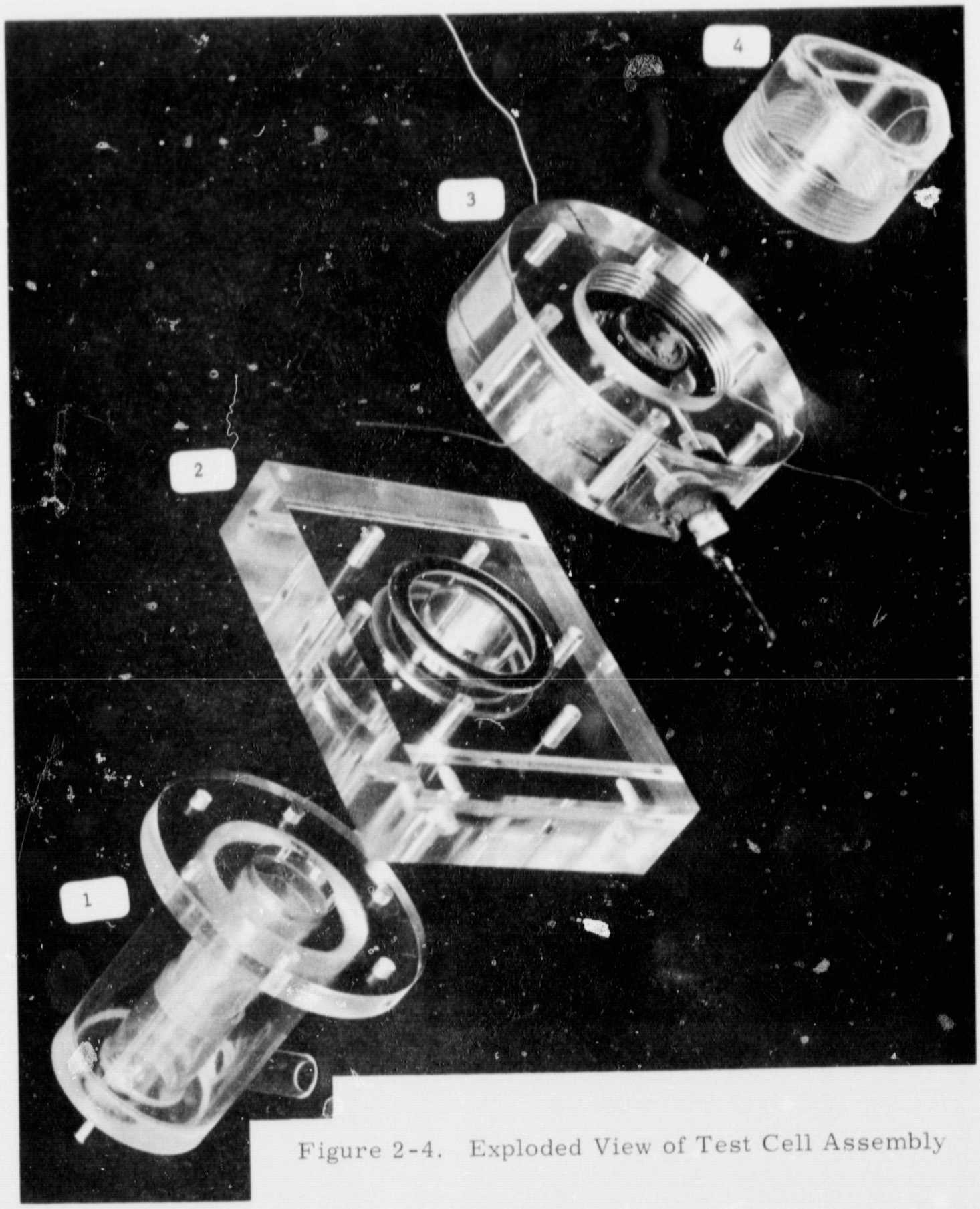


Figure 2-4. Exploded View of Test Cell Assembly

test electrode, the counter electrode and the reference electrode. The optical window, No. 4, permits the simultaneous illumination and magnified observation of the test electrode, positioned at the center of No. 3. Continuous electrolyte circulation from parts 3 and 4 through the mounting flange No. 2 and through the gas collector No. 1 guarantees clear optics and adequate gas-liquid separation at all times, regardless of gas pressure and gravity conditions (including 0-g).

The arrangement of electrodes inside part No. 3 is illustrated in greater detail in Figure 2-5. In order to permit the unencumbered optical examination of one 1/4" OD test electrode, positioned at the center, through the optical window, it was necessary to move the counter electrode out of the optical path, as indicated. The counter electrode holder, which determines the electrolytic current density distribution between the two electrodes has been given a shape consistent with the requirements of homogeneous current density at the test electrode and unobstructed illumination and observation from two angles of 15^{o} to the axis. A third electrode (zinc wire reference electrode) is positioned close to the test electrode, to measure more accurately its polarization during overcharge (gas formation) and during the two high rate discharges. Shown also is the electrolyte inlet pipe, which constantly sweeps electrolyte past the electrode to remove any gas bubbles emanating from the test electrode structure during overcharge and evacuation. A photographic top view of the cell mounting flange No. 3, showing the test electrode, the counter electrode, the 3 leads and the inlet pipe is shown in Figure 2-6.

Figure 2-7, an exploded view of the same electrode arrangement, illustrates further details. Fitted snugly inside the central cavity of the zinc test

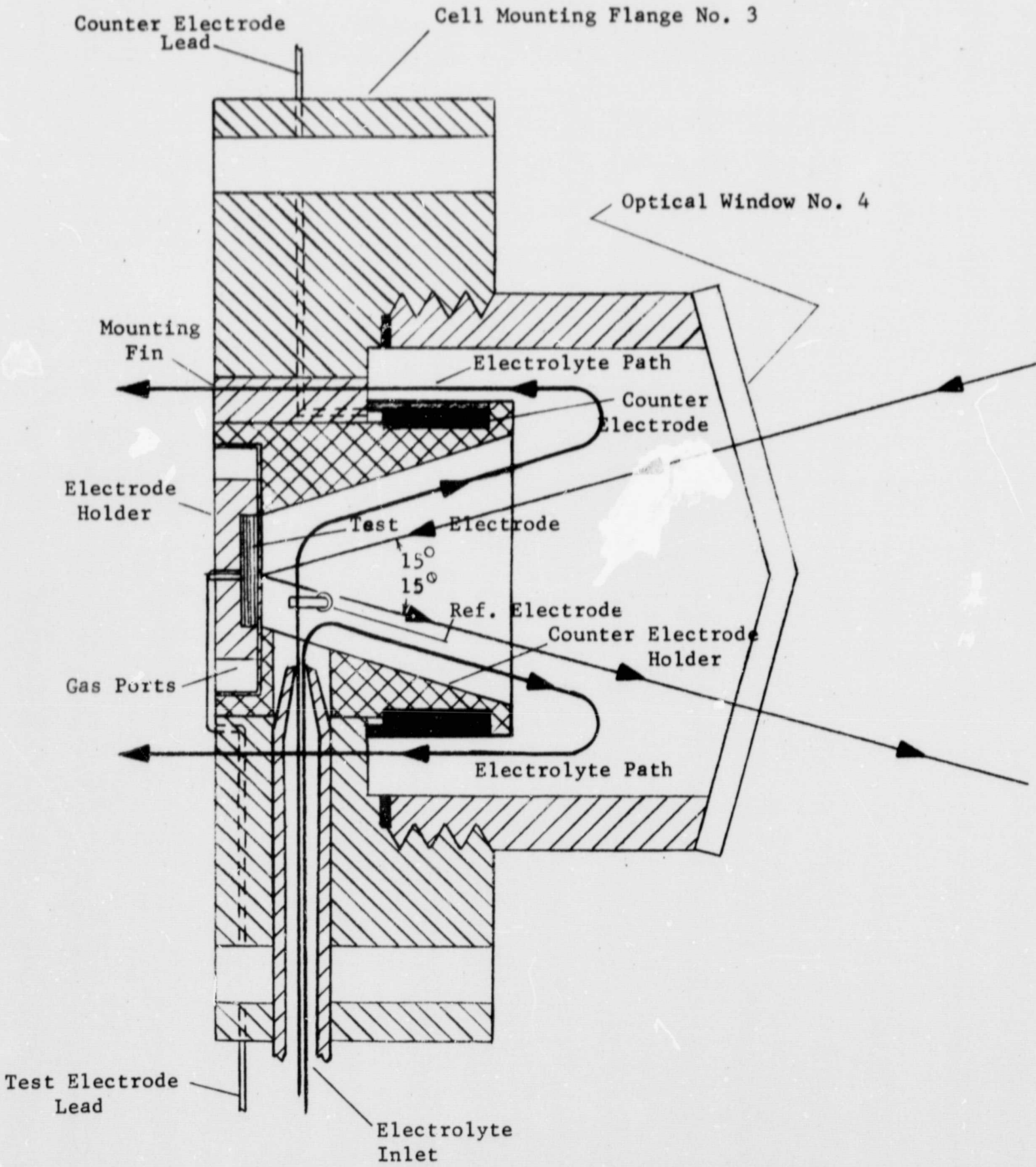


Figure 2-5 Details of Test Electrode and Counter Electrode in Task 2 Test Cell

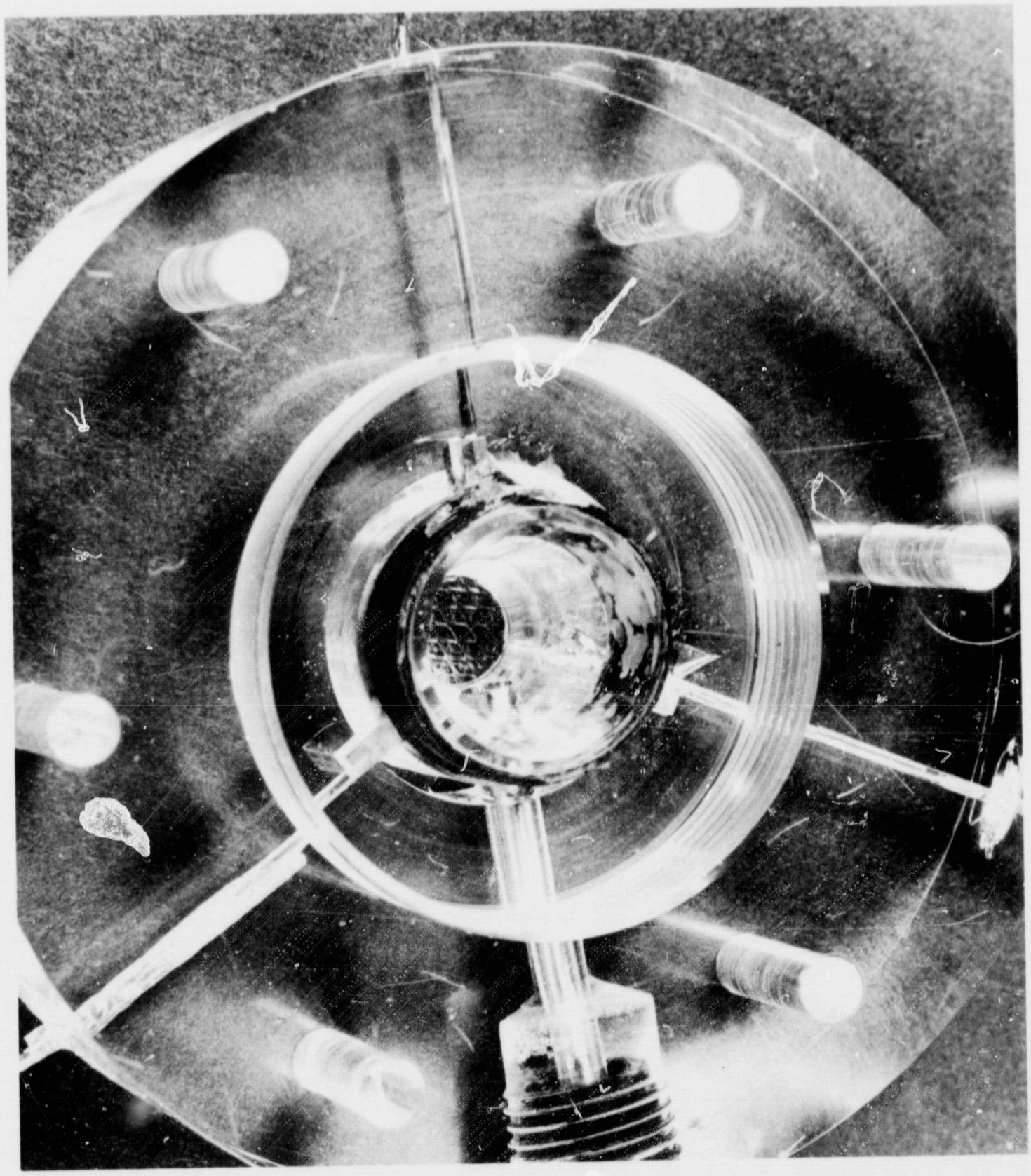


Figure 2-6. Top View of Cell Flange with 3 Electrodes and KOH Input Tube

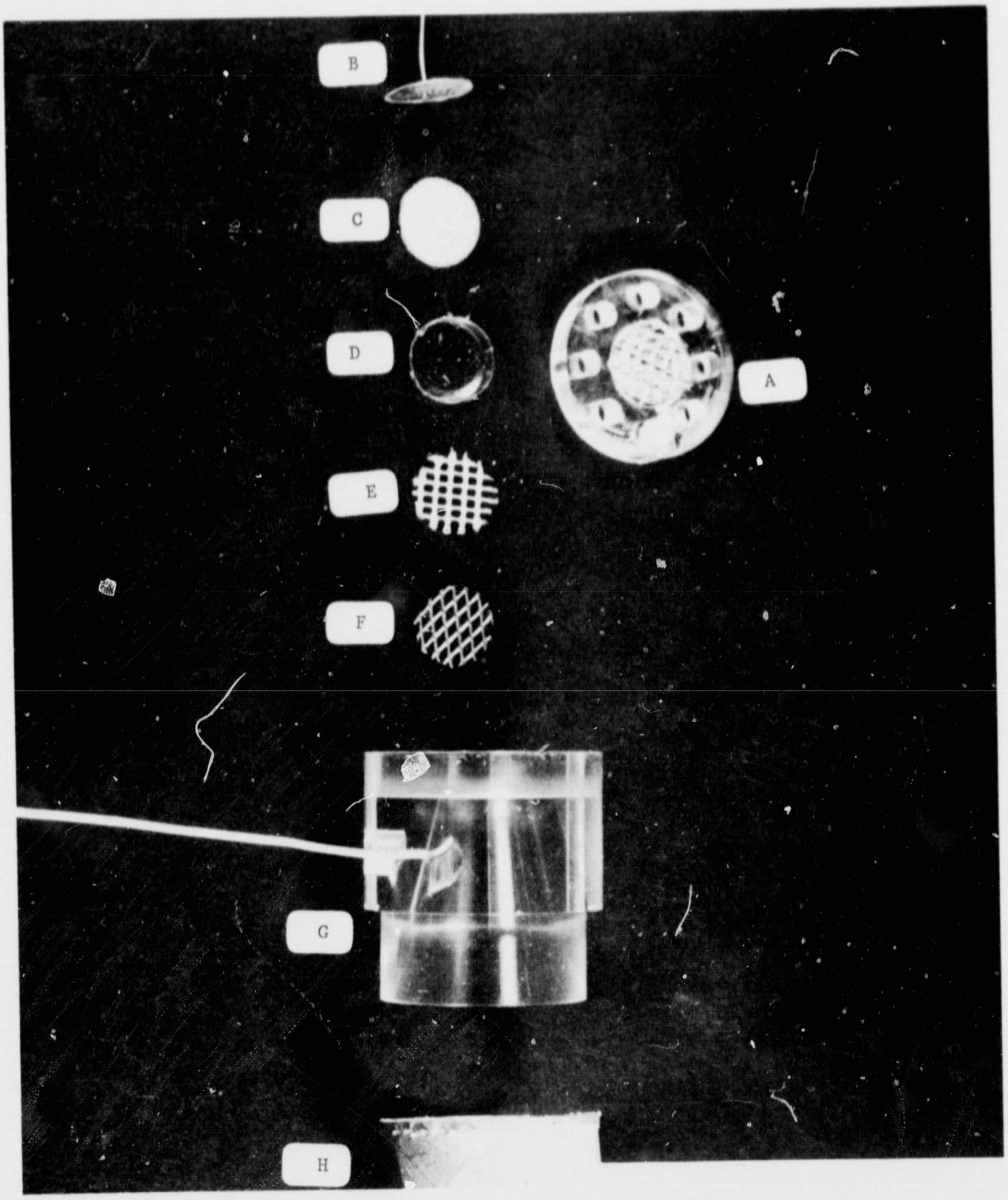


Figure 2-7. Exploded View of Electrode Arrangement

electrode holder A are the silver substrate B with lead, a 1/4" punching of a Yardney HR5 zinc electrode C, a membrane separator cup D (cellophane), a 1/4" punching of nylon Fablok E and a tight fitting punching of expanded nickel F to keep this multilayer sandwich pressed together. G is the counter electrode holder with reference electrode and H the silver-silver oxide counter electrode. Not shown in Figure 2-7 is the membrane separator cover for the counter electrode. A duplicate test cell structure is available for housing a silver oxide test electrode and a zinc counter electrode. In order to simulate zero gravity conditions as much as possible, it is planned to mount the two test electrodes in a horizontal position. However, with minor adaptations other orientations can be realized as well.

2.2.2 Gas Bubble Collection and Removal

The circulating electrolyte, mixed occasionally with gas bubbles, enters the gas collector part No. 1 (Figure 2-3) through the center and it leaves peripherally at the other end through the outlet tube. This forces the electrolyte to pass through the concentric screen shown. As a result of capillary forces any gas bubbles larger than the openings in the screen will be retained within the small cylinder. This gas collection process by means of electrolyte circulation is further illustrated in Figure 2-8, which includes various ancillary equipment and plumbing. A chemically inert centrifugal pump driven from a DC motor through a sealless magnetic coupling together with a metering valve provides electrolyte circulation, the flow rate of which can be adjusted.

Figure 2-8 also illustrates the auxiliary equipment needed for gas removal. This includes, in addition to the vacuum line or pump, a solenoid valve SV_1, for evacuation, two bleed valves BV_1 and BV_2 and a vacuum gage.

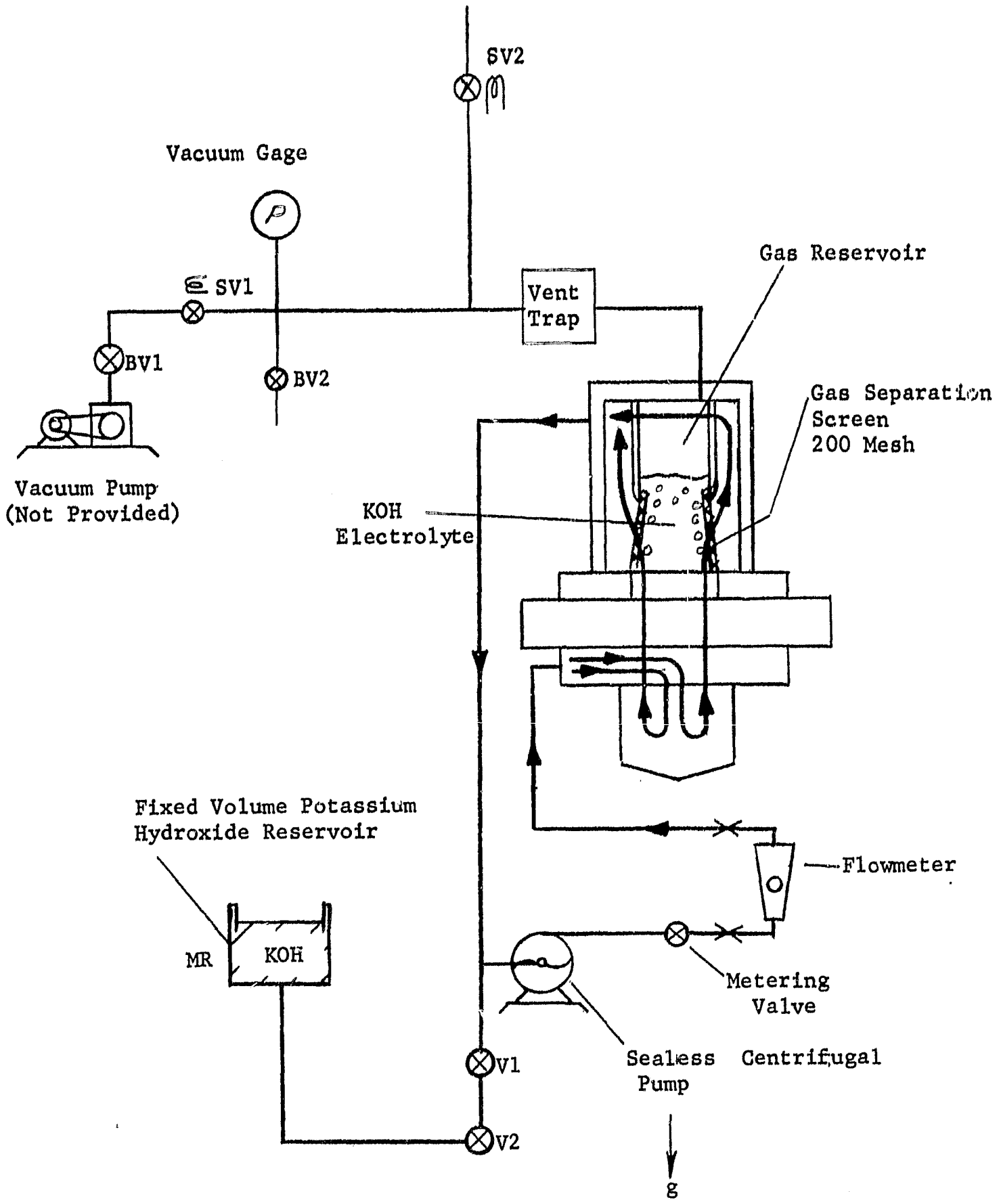


Figure 2-8 Auxiliary Equipment for Gas/Liquid Separation, Evacuation, Backfill and Activation

Without the bleed valves (BV_1 wide open and BV_2 closed) evacuation of the system by means of SV_1 would rapidly proceed to an absolute pressure of approximately 5 mm Hg at which the electrolyte begins to "boil". Such boiling may become very violent, leading to the entrainment of electrolyte into the vacuum system. A judicious permanent throttling adjustment BV_1 and opening of BV_2, on the other hand, will prevent such boiling and slow down evacuation sufficiently to guarantee proper gas removal without entrainment. After closing SV_1, the permanent "leak" in BV_2 will automatically "backfill" the system. Since the total gas volume is very small, this simple method of backfilling looks very promising. Nevertheless, a separate automatically programmed solenoid backfill valve SV_2 is provided as a standby. BV_2 takes care of still another function. It also prevents pressure build-up during overcharge.

At the end of the first discharge D_1, it is now desired to remove all trapped gas from this system, including that inside the test electrode. Thus the solenoid valve to the vacuum line is activated. Although many gas bubbles may traverse the gas-liquid interface inside the gas reservoir during the gradual evacuation step, the liquid level rises only a little and only temporarily. Two bleed valves are provided to prevent violent "boiling" of the electrolyte at very low pressures ($\sim$5mm Hg). After closing the vacuum valve, the system can now be refilled to ambient atmosphere by means of the backfill solenoid valve. The bleed valve will automatically perform the same function at a slower rate. This evacuate-backfill cycle is repeated a second time to reduce the trapped gas volume inside the test electrode to an insignificant value. The second discharge D_2 in the absence of trapped gas can now commence.

For maximum reliability the use of two entirely separate electrically isolated systems, one for the zinc and one for the silver test electrode is recommended. With the exception of a common vacuum connection, all items illustrated in Figure 2-8 must, therefore, be duplicated.

2.2.3 Activation

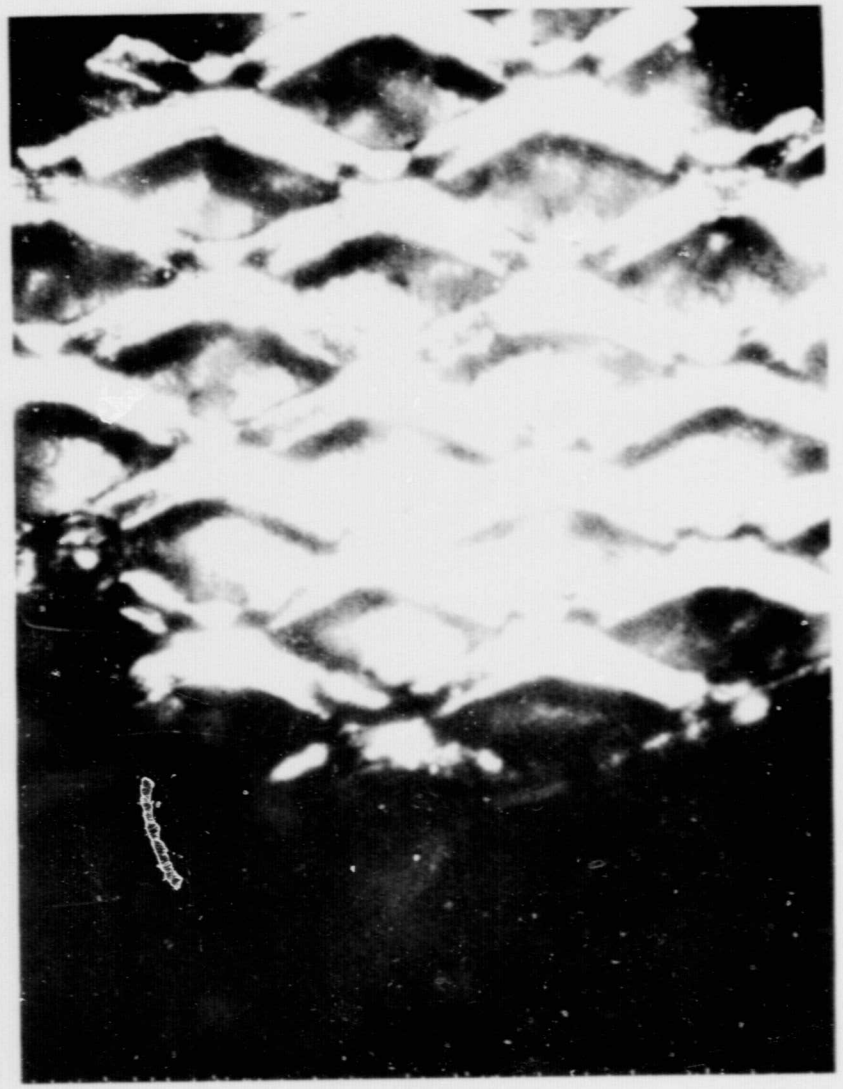
For the purpose of activation prior to the test sequence, a manually operated valve V_1 in series with a metering valve V_2 is used, which connects a metered reservoir MR filled with 45% KOH to the system. Activation must be preceded by an evacuation step and the amount of KOH dispensed slowly from MR must be carefully adjusted to bring the gas-liquid interface inside the gas reservoir to the proper level. In spite of the slowness of the filling process, gas bubbles may become mixed with the entering KOH. For this reason the centrifugal pump should have been turned on earlier to insure proper gas-liquid separation during filling. After closing SV_1 and backfill, the system is now ready for testing.

2.2.4 Optical Detection of Trapped Gas, Illumination and Photography

As stated earlier the optical detection of small gas bubbles present inside the three-dimensional and highly porous structure of a commercial silver or zinc electrode through a transparent membrane separator is virtually impossible because such electrodes are opaque. Fortunately the distribution of such very small isolated gas bubbles is not likely to "block-off" significant areas of the test electrode, which could lead to electrode passivation. On the other hand, larger aggregates of gas bubbles at the electrode-membrane interface can prevent the localized passage of ionic current flow, if these aggregates join together to form "pancake-type-structures" devoid of electrolyte. Such structures have indeed been detected on all test electrodes

studied so far. Since these gas pancakes are in contact with one of the membrane separator surfaces, their optical detection can be enhanced by using a narrow beam type of illumination, the specular reflection on the membrane surface of which is picked up preferentially by the microscope objective or camera. Under these conditions the gas pancakes show up as bright spots and their visibility is improved considerably. Although this contrast enhancing effect was discovered earlier during our exploratory investigations no photographic records were made at that time. Figure 2-9 shows a pair of such photomicrographs at a magnification of 17 which refer to the new zinc test electrode shown in Figure 2-6. They were made with improvised optical equipment. The left-hand picture of Figure 2-9 illustrates the gas loaded condition with many bright patches visible, wherever the trapped gas is located. The righthand picture shows the same electrode after gas removal. As can be seen, many of the bright spots have disappeared.

This specular reflection feature has been incorporated also in the design of the auxiliary equipment for automated photography, illustrated in Figure 2-10. As shown, two electronic flash tubes, mounted perpendicularly to the optical plane (this position not shown in Figure 2-10) at a 15^{o} angle of incidence, illuminate the two test electrodes at the proper angle. Scattered and reflected light from the gas pancake-membrane interfaces enters lenses A and B to be focused and enlarged three times on the film plane of the 35mm camera. Images of the two 1/4 OD test electrodes, 4 1/4" apart, are formed side by side on a single frame of film with a black metal septum positioned in between to prevent any of the rays from one object from falling on the other image. Since in this arrangement the plane of the two test electrodes and of the film are parallel, there should be no difficulty in achieving proper focusing for the entire electrode areas. It is planned to use

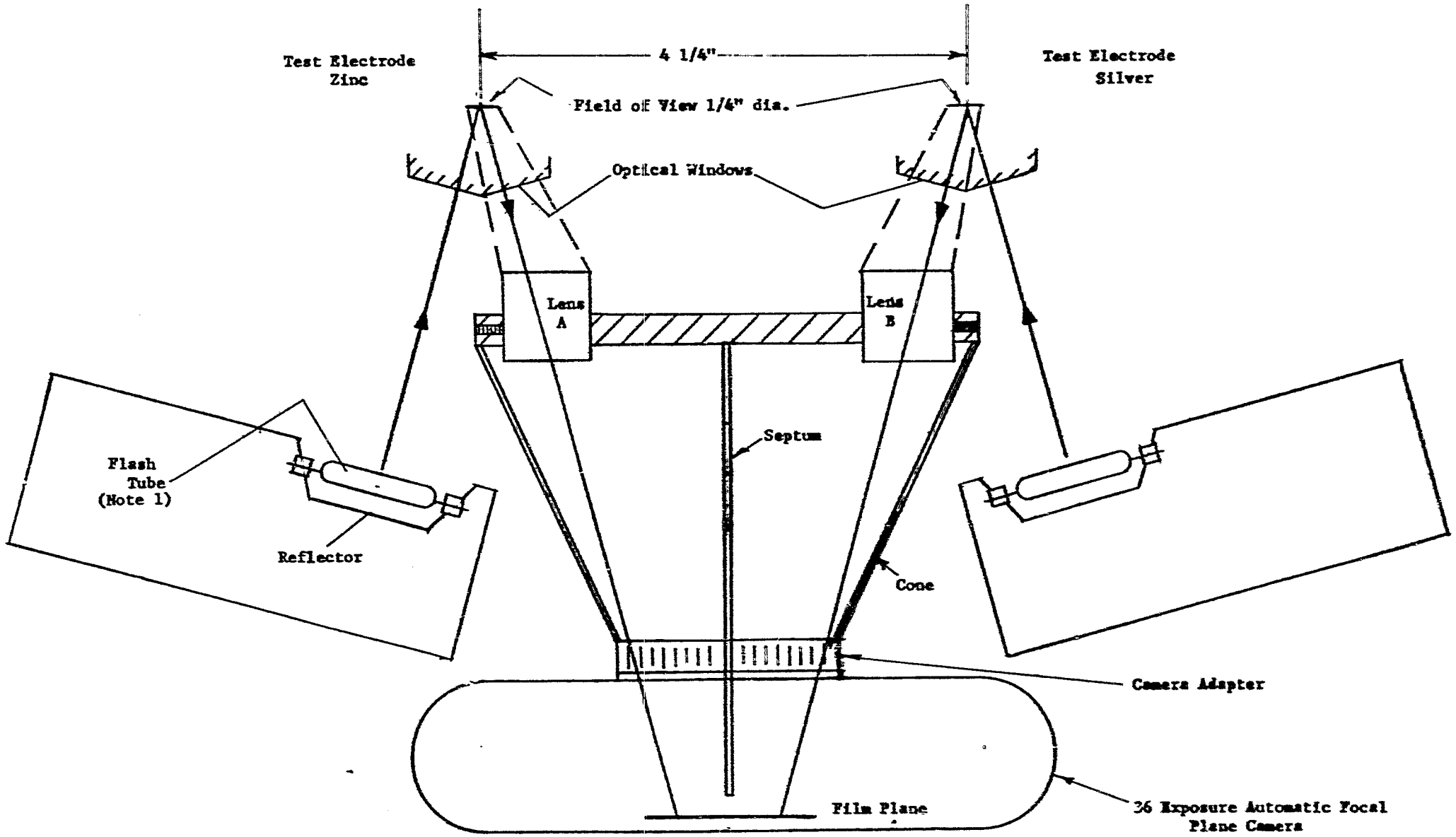


Gas



No Gas

Figure 2-9. Photomicrograph of Zinc Test Electrode



NOTE: Flash tube shown rotated 90°
from actual position

Figure 2-10 Camera and Test Cell Arrangement for Task 2

standard color film cartridges of 36 exposures. This equipment will be built and tested during the next quarter.

2.3 Preliminary Results

During the month of June 1968 one of the two new test cells, equipped with a zinc test electrode and a silver oxide counter electrode, was subjected to various manual testing procedures. Although the circulating electrolyte feature by means of a centrifugal pump was included, the plumbing, evacuation technique and optics used were simplified versions of the test plan system described earlier. Since the basic differences between the old and the new cell constructions are in the fluidics rather than the electrochemical areas, special attention was given to electrolyte circulation, the accumulation and transport of gas bubbles during overcharge and evacuation, the separation of gas bubbles from the electrolyte stream and the removal of gas from the system.

At that time a 200 mesh stainless steel gas separation screen was used in part No. 1. Except for the smallest bubbles the removal of gas from the electrolyte was quite efficient. Since the openings in a 200 mesh screen are 0.0029" large any gas bubbles below 0.003" OD will not be removed. However, the circulation of such small bubbles did not interfere in any way with the proper functioning of the cell.

Although gas separation is easiest with the test electrode in the horizontal position, near vertical orientations have also been found to perform satisfactorily. However, in this mode the constraints on the permissible gas volume stored inside the cell is more critical. The proper adjustment of the electrolyte flow rate was found not to be critical. A rate of approximately one liter per minute is satisfactory. Gas producing contaminations of the zinc electrodes made their appearance in the new

test cell after approximately 10 hours of operation. This contamination was particularly noticeable at the zinc reference electrode. For this reason it was decided to encapsulate all electrodes inside membrane separators.

The discharge performance of the zinc test electrode and its D_2/D_1-ratio were found to be compatible with earlier findings.

2.4 Conclusions and Recommendations

The design features and experimental test data obtained on this task so far are sufficiently encouraging and detailed to permit an adequate formulation of the test plan. This has been covered elsewhere.

As the approved test plan is being implemented, further testing of the individual zinc and silver electrode systems will be necessary. This is particularly applicable to the silver test electrode system which so far, has not been given as much attention as the zinc electrode.

3.0 Task 3 - Testing of Commercial Secondary Silver-Zinc Cells

3.1 Introduction

The purpose of the bench top testing of the Task 3 commercial cells was to try and determine the cell degradation that may be expected of a cell under stress. This degradation was to be caused by discharging the cell to a given depth of discharge during the stress portion of the proposed test sequence. The depth of discharge was to be adjustable from 40% to 65% of rated capacity. During any one test sequence on a given cell, the depth of discharge was constant.

Initial tests were run on a Task 3 cell where the depth of discharge was to the 35% level. The cell showed a 12.9% loss in capacity. The measurements for this initial test were made by hand. The results indicated that further testing at greater depths of discharge would be necessary to further characterize the commercial cell. Increased cell degradation would result from either increasing the number of stress cycles or from increasing the depth of discharge during the stress cycle, or both. Since the test sequence was fixed, the depth of discharge was increased. The tests are very time consuming so they were run automatically on a bench top model of the proposed logic circuitry for the breadboard. This manner of testing not only tests the cell but also provides an opportunity to try the types of circuits that will be used on the breadboard. The primary objective was to show significant degradation in one test sequence.

The test sequence is the same as is given in Table 3-1 of Quarterly Report No. 1. This sequence is repeated here in Table 3-1 with a change in nomenclature that has recently been adopted.

In all tests, the capacity discharge rate was 5 amps and the capacity charge rate was C/10 or 500 ma. The stress discharge was set to give the

desired depth of discharge in a 30 minute time period. The stress charge was adjusted so that the cell could be fully recharged in about 45 minutes.

Table 3-1 Preliminary Task 3 Test Sequence

1. Stress Charge
2. Capacity Discharge
3. Capacity Charge
4. Polarization Discharge
5. Polarization
6. Stress Charge
7. Stress Discharge
8. Stress Charge
9. Stress Discharge
10. Stress Charge
11. Stress Discharge
12. Stress Charge
13. Stress Discharge
14. Stress Charge
15. Stress Discharge
16. Stress Charge
17. Polarization Discharge
18. Polarization
19 Stress Charge
20. Capacity Discharge
21. Capacity Charge

The first step of the sequence in Table 3-1 caused some difficulties. This step was a stress charge of a new nearly fully charged cell. Under these

test conditions, the cell would accept no charge at all and appeared to have a very high impedance. The result was an immediate transition through the first test step and into the second. Because of this effect, the cell could not be made to accept the charge to make sure that the cell was, in fact, fully charged. This situation is overcome by the change in test sequence that is discussed in Section 3.3.

The equipment for these tests is as described in Section 3.3.2 of Quarterly Report No. 1.

3.2 Test Results

To date, three cells have been automatically tested at various depths of discharge and for various numbers of complete test sequences.

The first cell was tested at a 40% DOD for one complete test sequence. The second cell was tested at 65% DOD for one test sequence though the sequence was preceeded by three capacity measurements caused by logic malfunction that was later corrected. The third cell was tested at a 65% DOD level for a total of five complete test sequence.

The tests on the first cell at 40% DOD showed very little degradation when comparing the initial and final capacity measurements. The initial capacity was 6.70 amp-hrs. and the final capacity was 6.40 amp-hrs. The percentage degradation was about 4.5%.

The cell polarization tests employed a current ramp that had a maximum value of 8.5 amps. The cell voltage at the end of the second polarization was about 30 mv lower than the voltage at the end of the first polarization. In general, the tests at 40% DOD demonstrated that this level of discharge was too low to cause significant cell degradation for this test sequence.

Cell number two was tested with the stress cycles set for 65% DOD. At this level, the noise generated by the stress charge relay upset the logic so that three false starts occurred before the cause of the noise was found and corrected. The three false starts consisted of essentially a capacity discharge and recharge. After the initial false starts, a complete test sequence was run. In all, there were five capacity measurements made. Three were the result of the false starts and two were part of the test sequence. The measured capacities are as follows:

1. 7.81 amp-hours
2. 7.81 amp-hours
3. 6.72 amp-hours
4. 7.50 amp-hours
5. 5.78 amp-hours

All of the capacity measurements were preceeded by a stress charge. All capacity discharges were recharged at C/10 rate.

There is definite cell degradation noticeable from these measurements. If the degradation is calculated from measurements 4 and 5, the result is about 23%. The current limit for the polarization measurement for this sequence was set for a maximum of 15 amps. The cell voltage at ramp cutoff was about 35 mv lower for the second ramp compared with the first.

The third cell was also used with stress levels set for 65% DOD. Because of the possibility that the rate charge that preceeds the capacity measurement might have a significant effect on the capacity, an experiment was made with this cell to determine this. This cell was tested according to the normal test sequence. In addition, a third capacity measurement was made after the test sequence which was preceeded by a C/10 charge rate. The end of the measurement consisted of two capacity measurements one preceeded by a stress

charge and one preceeded by a C/10 charge.

The initial cell capacity was 8.19 amp-hrs. The final capacity was 7.07 amp-hrs. for a 13.7% degradation. The third capacity measurement has a value of 8.32 amp-hrs. which was even slightly greater than the initial capacity.

These measurements tend to indicate that the rate of charge that preceeds a capacity measurement can have a significant effect upon that measurement.

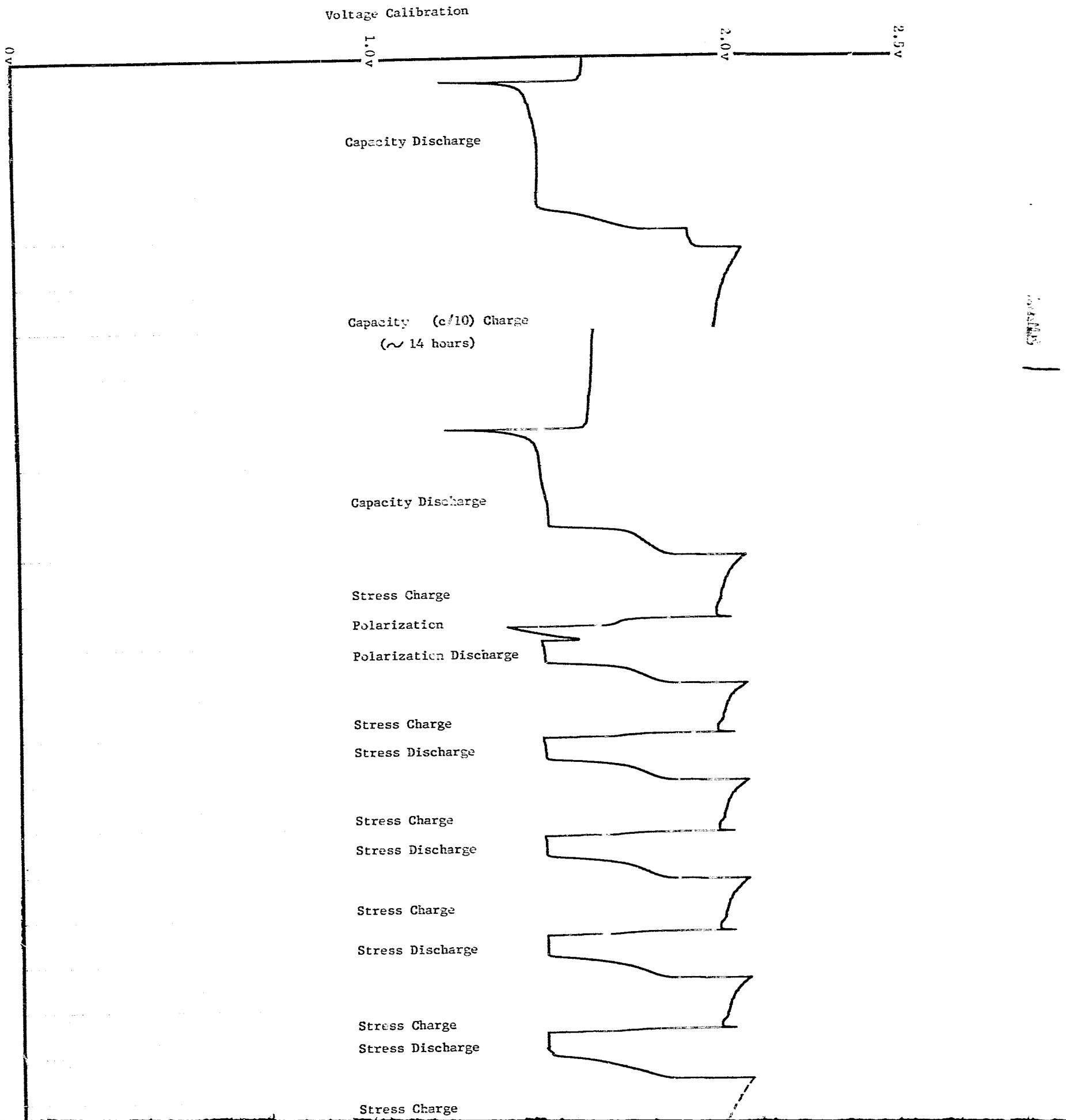
Cell three was run through four additional test sequences in order to show as much cell degradation as possible. The capacity measurements for these tests are summarized below. A period of about 3 weeks elapsed between sequences 1 and 2. The overall degradation from first measurement to last was 61.8%.

The cell voltage plots for these five test sequences are shown in Figure 3.1 to 3.5.

Sequence	Capacity			%Degradation
	Initial	Final	Additional	
1	8.19	7.07	8.32	13.7
2	6.40	5.94	-	7.2
3	7.18	4.85	-	32.4
4	6.57	3.59	-	45.5
5	5.47	3.12	-	43.0

3.3 Discussion of Test Results and Recommendations

The data of cell three indicates fairly clearly that the history of a cell preceeding a capacity measurement has a significant effect on that measurement. It is also fairly clear that the stress cycles of the proposed test sequence (at the 65% DOD level) do not show much cell degradation if both


Voltage Calibration
0 v
1.0 v
2.0 v
2.5 v
Capacity Discharge
Capacity (c/10) Charge
(~ 14 hours)
Capacity Discharge
Stress Charge
Polarization
Polarization Discharge
Stress Charge
Stress Discharge
Stress Charge
Stress Discharge
Stress Charge
Stress Discharge
Stress Charge
Stress Discharge
Stress Charge

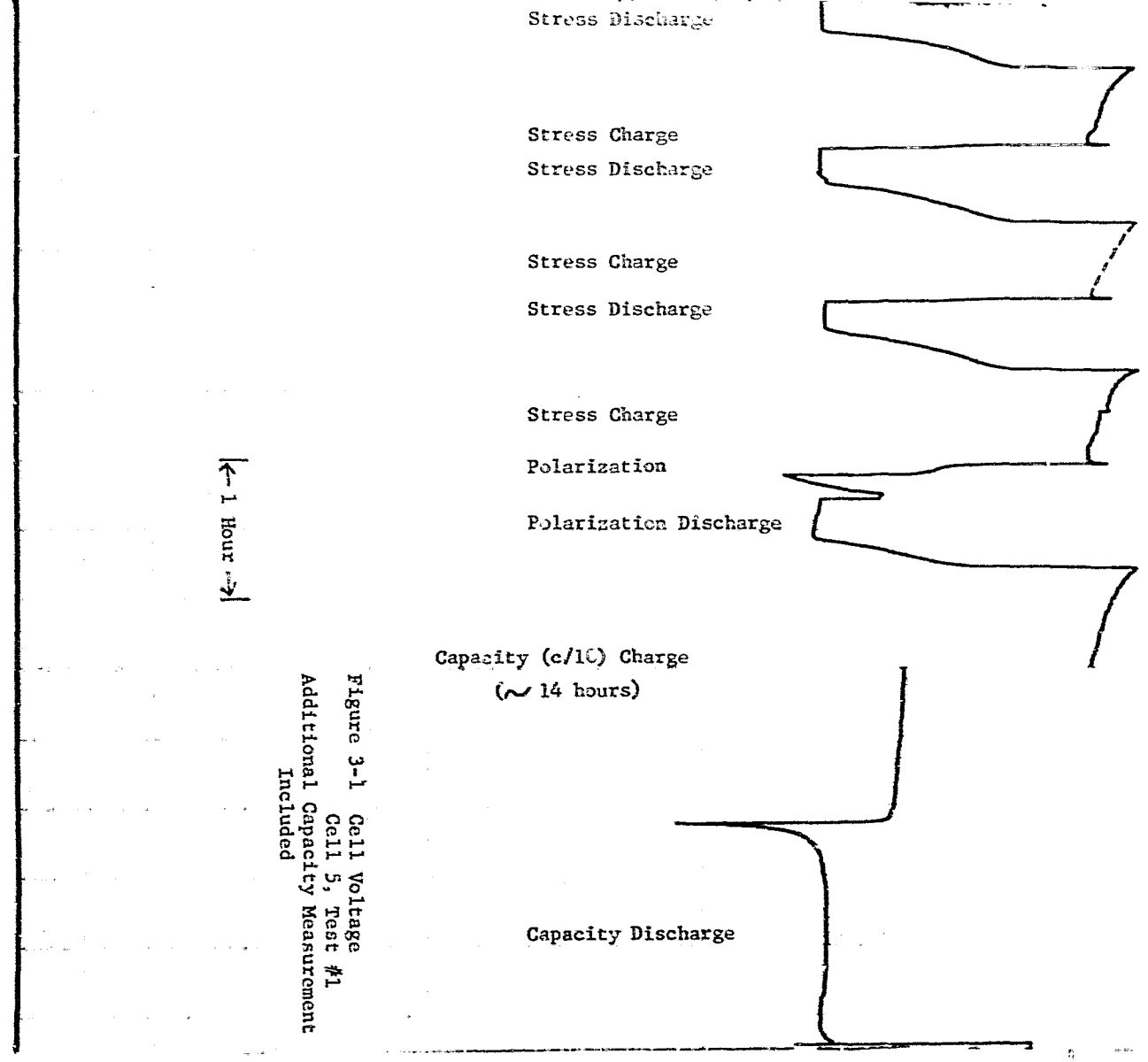


Figure 3-1 Cell Voltage
Cell 5, Test #1
Additional Capacity Measurement
Included

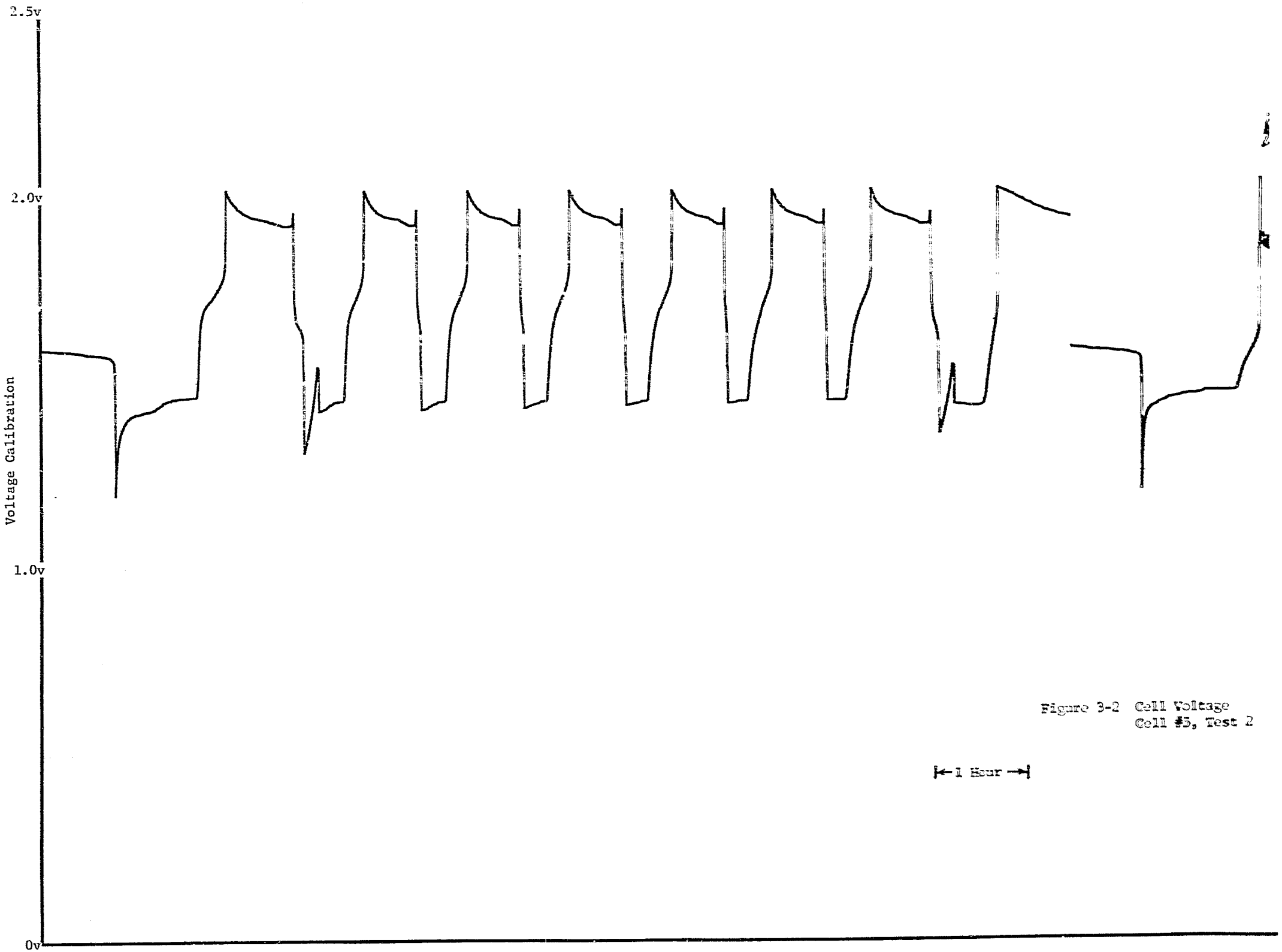


Figure 3-2 Cell Voltage
Cell #5, Test 2

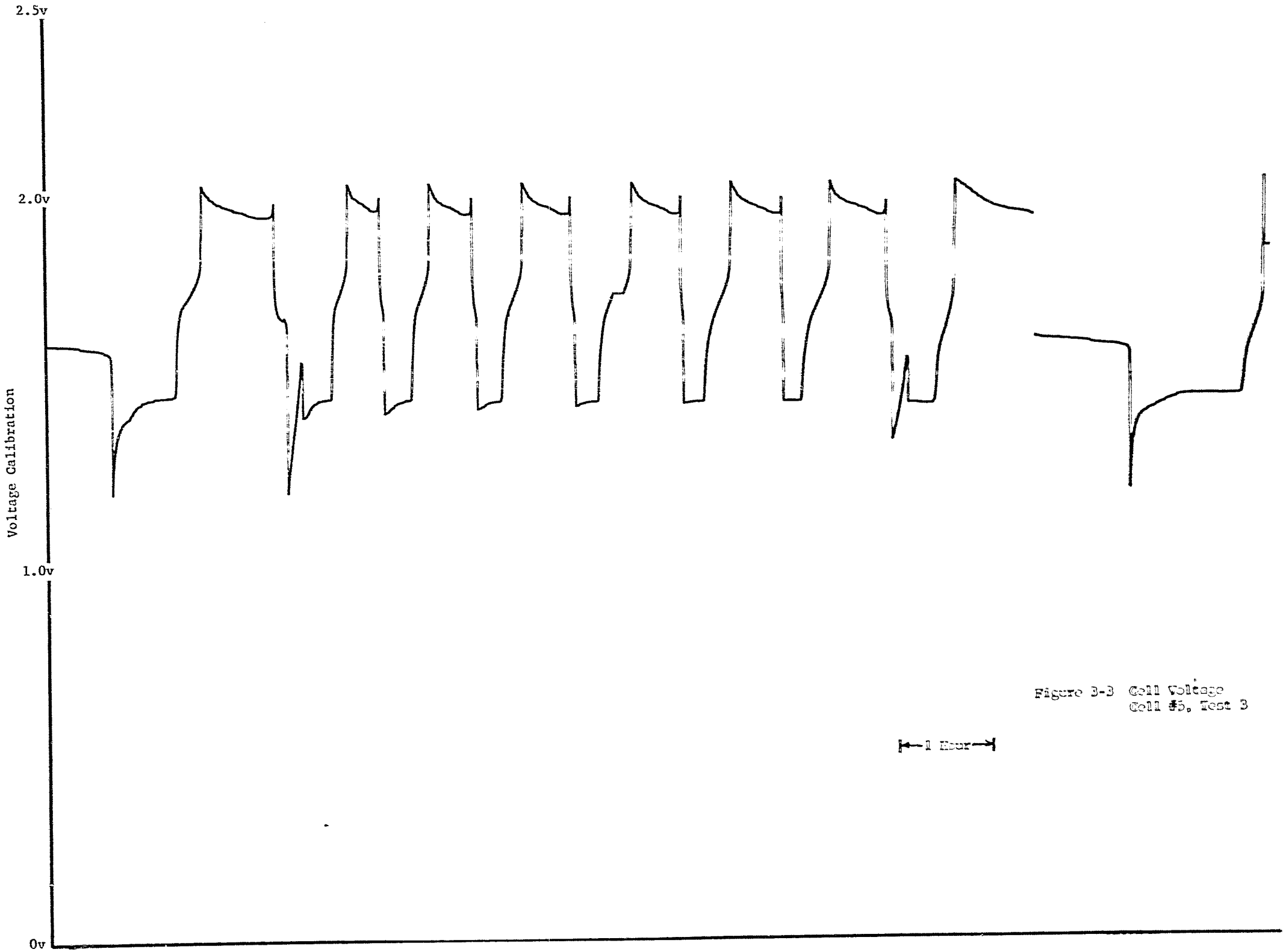


Figure 3-3 Cell Voltage
Cell #5, Test 3

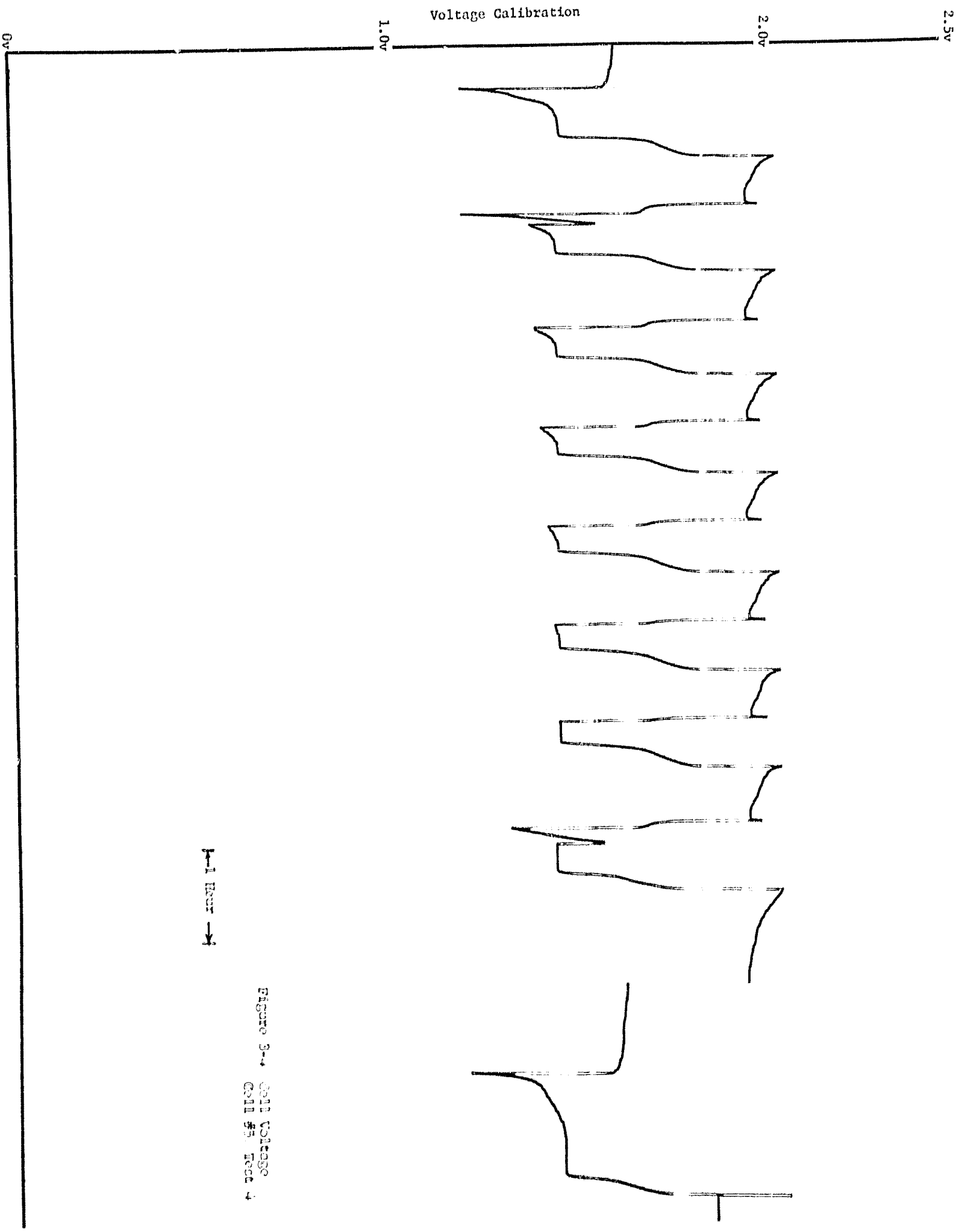
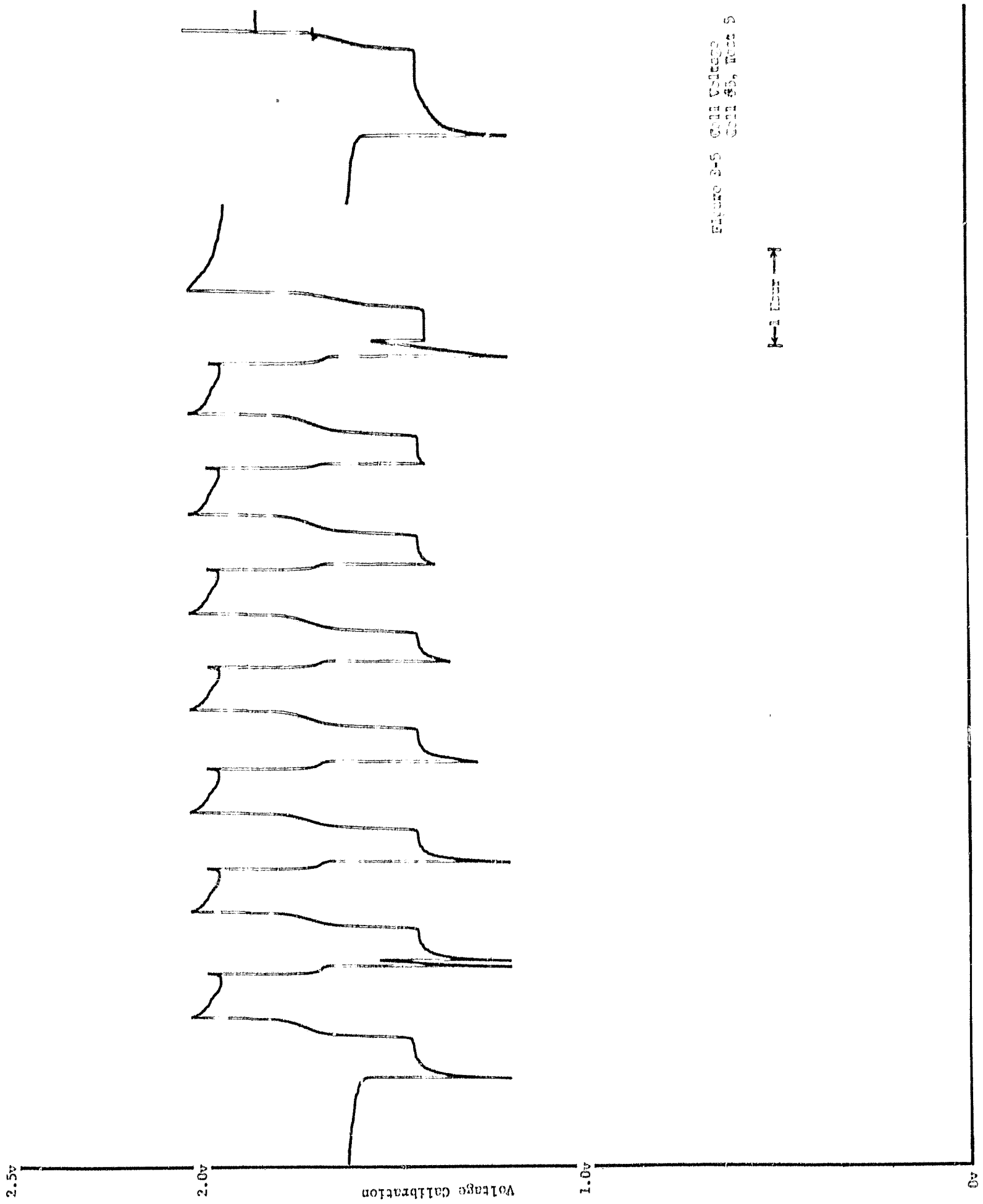


FIGURE 3-4 CELL CURVES
CELL #5 ECG 4


Voltage Calibration
2.5v
2.0v
1.0v
0v

FOLDOUT FRAME: 2

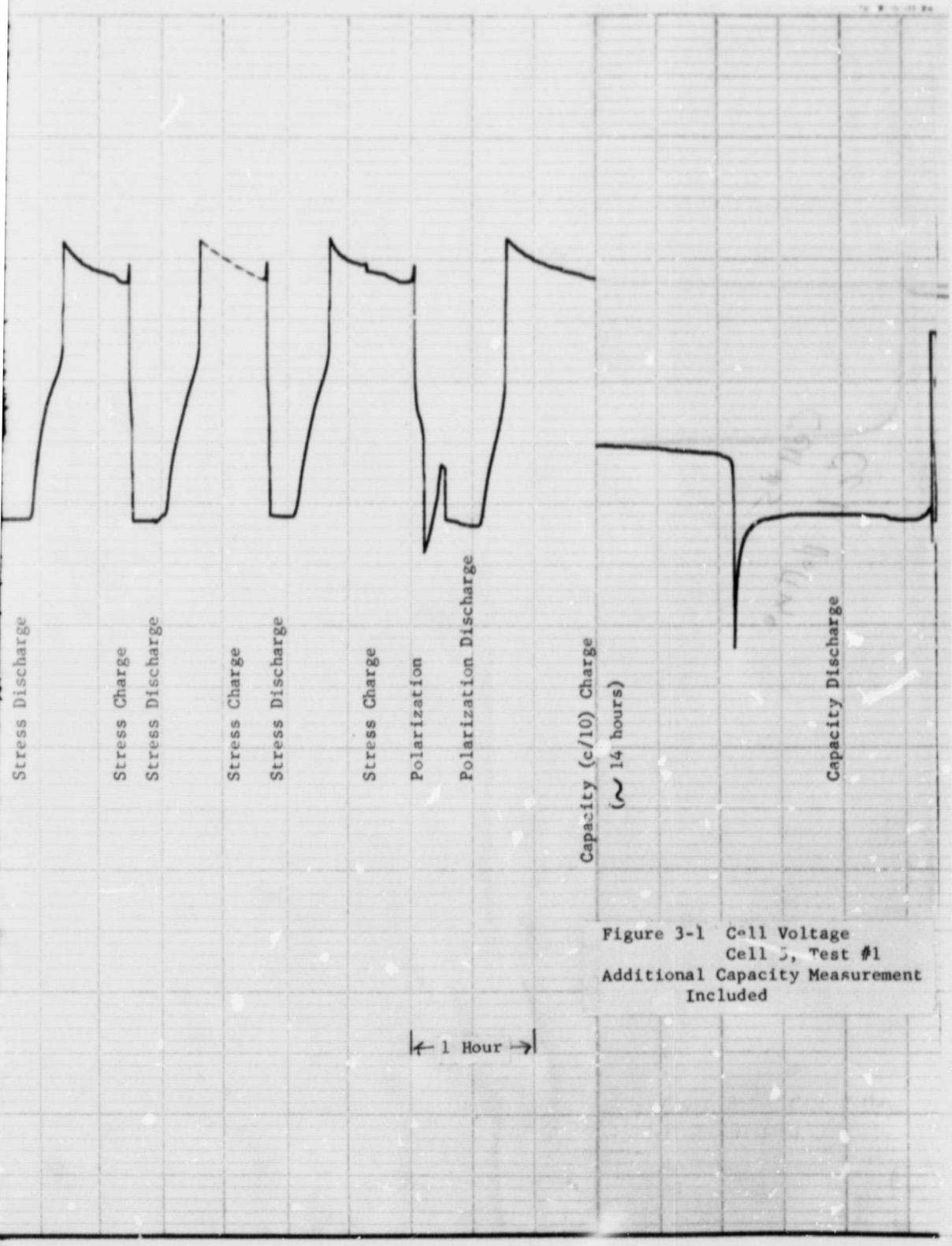


Figure 3-1 Cell Voltage
Cell 5, Test #1
Additional Capacity Measurement
Included

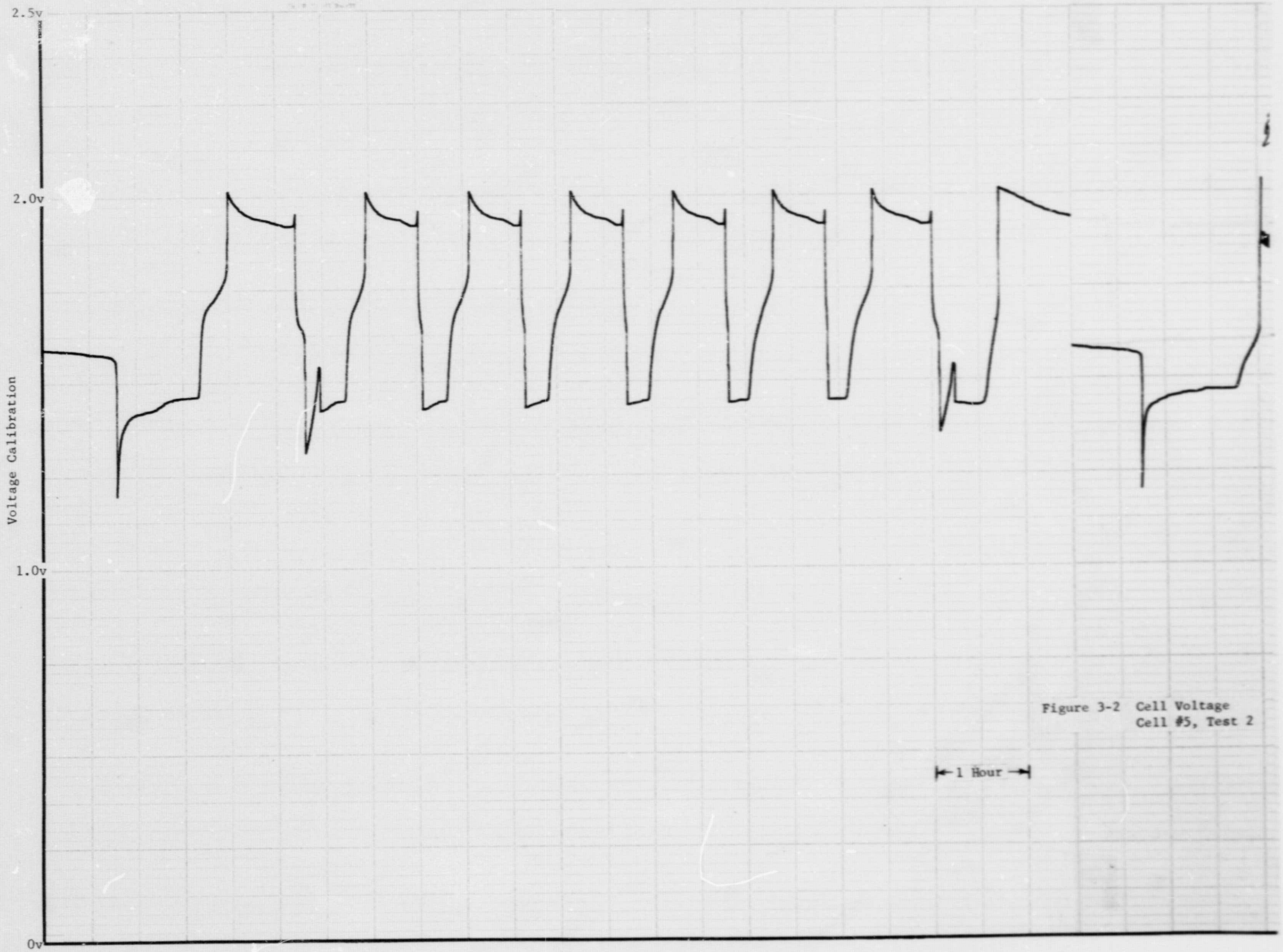


Figure 3-2 Cell Voltage
Cell #5, Test 2

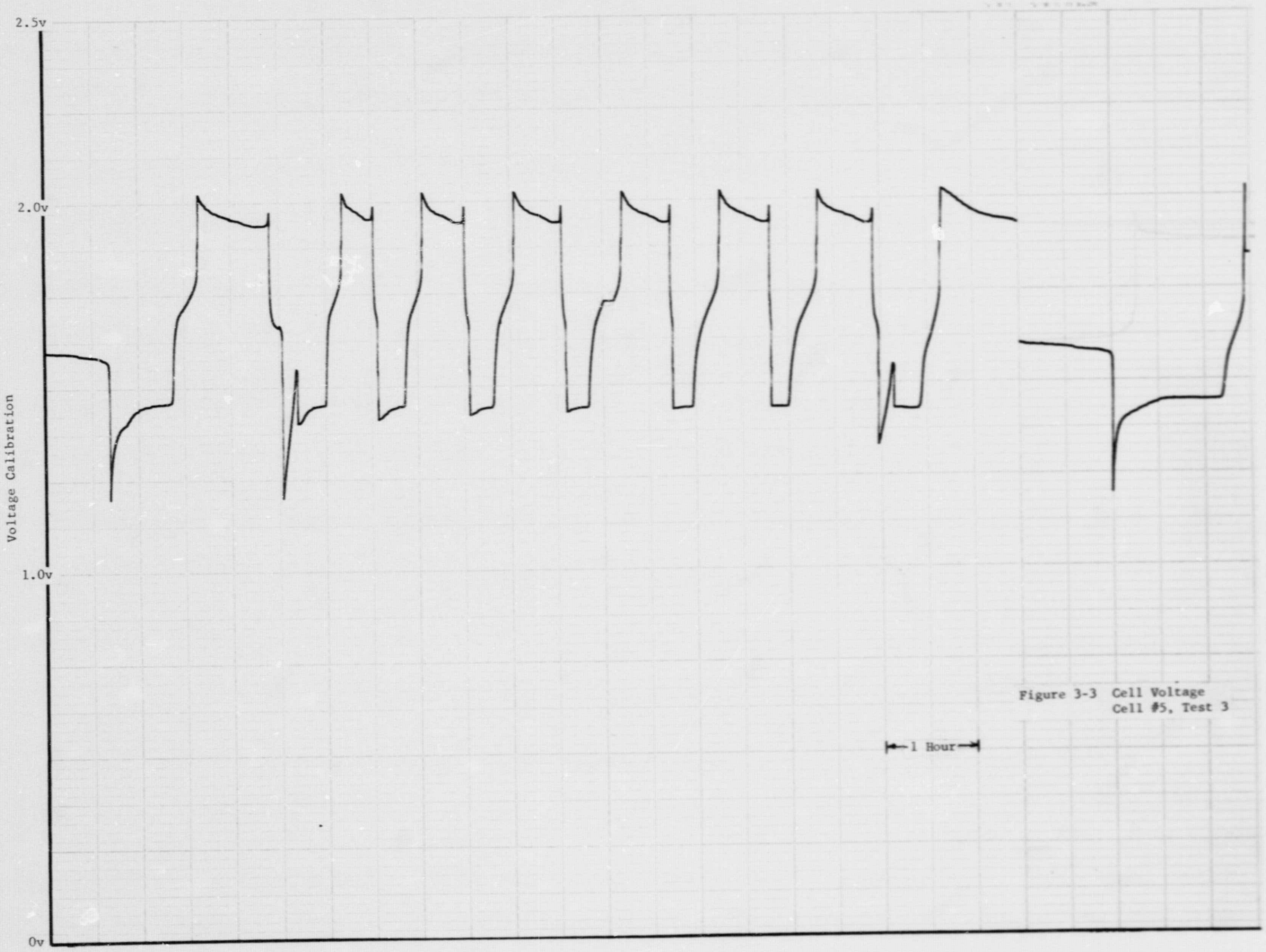


Figure 3-3 Cell Voltage
Cell #5, Test 3

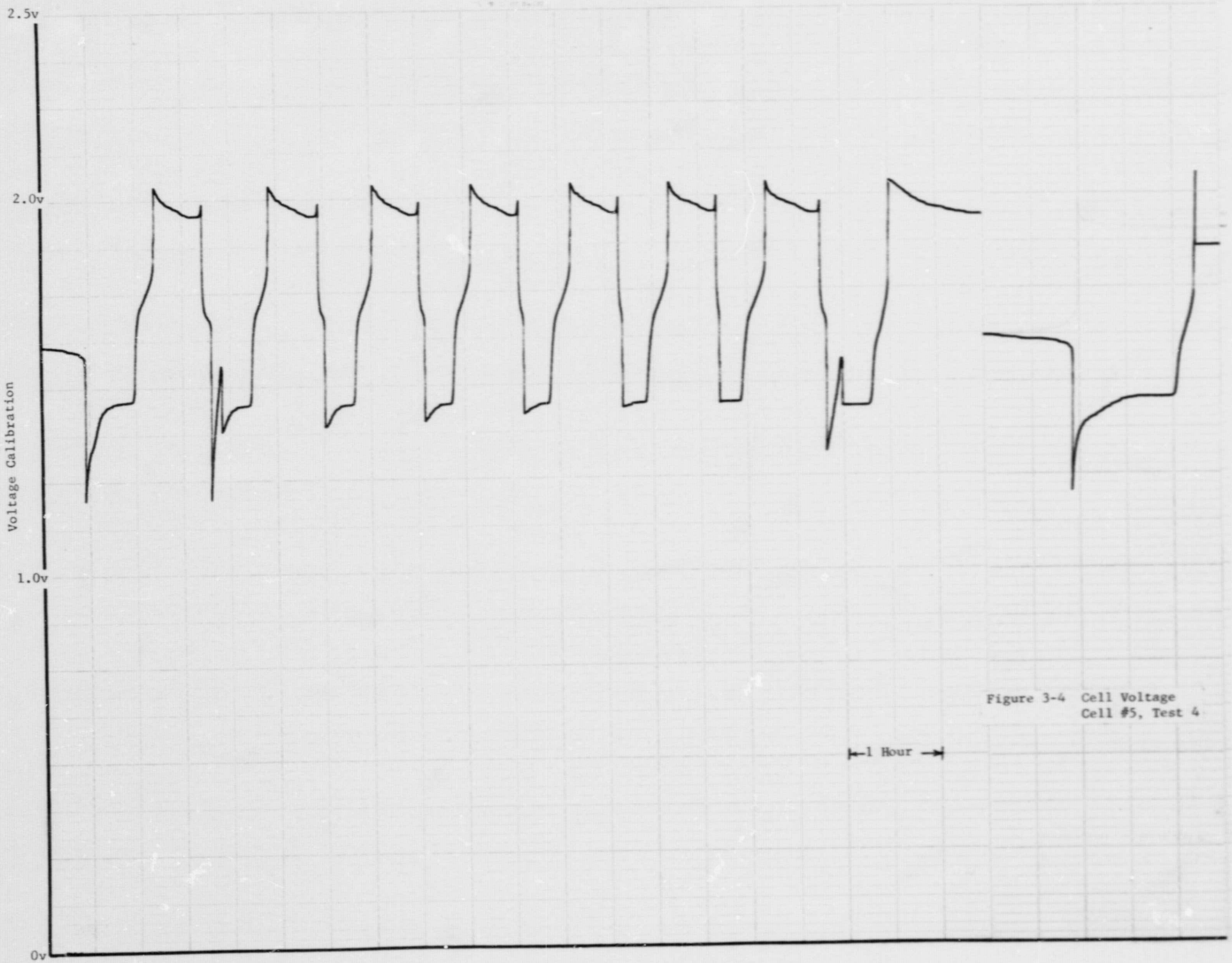


Figure 3-4 Cell Voltage
Cell #5, Test 4

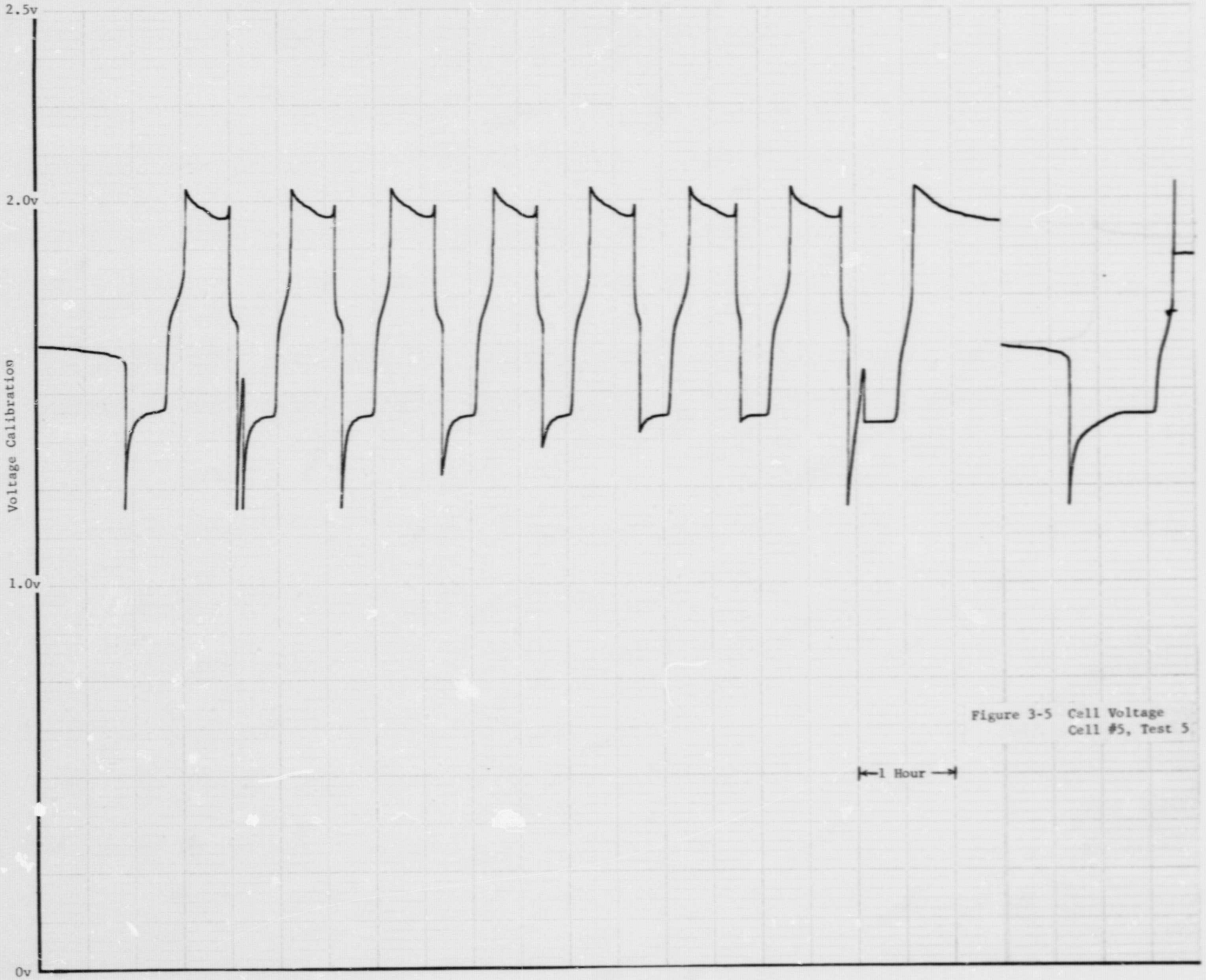


Figure 3-5 Cell Voltage
Cell #5, Test 5

capacity measurements are preceeded by a C/10 charge.

For these reasons, two changes have been incorporated into the test sequence. First, the overall sequence has been changed to the one shown in Section 4-1 of the Test Plan. The initial stress charge is eliminated and is replaced by a stress discharge and capacity charge. The stress charge immediately preceeding the final capacity measurement is replaced by a capacity charge. So that the overall time to complete the sequence is not drastically lengthened, the final charge is eliminated and the cells remain in an uncharged state.

The second change is the recommendation that the capacity charge rate be increased from the C/10 rate that is used now. A rate of C/5 to 2C is recommended. The changes in the test sequence should provide more meaningful data on the Task 3 cells.

In order that significant degradation be apparent during one test sequence, the breadboard will be capable of very high depths of discharge, to capacity if necessary. It must be realized, however, that these high levels will cost either time or power consumption or both on the stress charge.

It would also be possible to run a cell through more than one test sequence though not on a completely automatic basis. The cells would have to be recharged by hand and then restarted through the test sequence. This procedure is to be recommended if very high depths of discharge are undesirable.

SECTION III - CONCLUSIONS

A series of twelve tests to determine LCD of pure zinc electrodes using the current ramp approach has demonstrated that this method is capable of very reproducible results. With a current ramp slope of 62 ma/min. which approximates the test conditions of Arcand's previous work at JPL, the LCD value measured in three separate tests fell within $\pm$2% of the average. Most scatter was encountered with horizontally oriented electrodes tested with 7 ma/min. ramp slope. In this case the results of three tests fell within $\pm$7% of the average. Based on these results, it is concluded that the use of six sample cells in the breadboard is an adequate degree of replication for this experiment.

These tests also demonstrated the significance of discharged capacity on the LCD value obtained in a measurement. They point up the necessity for a careful selection of current ramp slope in order to make the most meaningful comparison of LCD values made under different test conditions such as 1-g vs. zero g.

The significant effect of g-level on a cell of this design has been demonstrated by the large differences in LCD values obtained when electrode orientation was changed from the vertical to a horizontal position to suppress convection. LCD values decreased by 25% for the horizontal position (simulating zero-g) compared to the vertical tested at identical current ramp slope. When ramp slope was adjusted to give a similar discharged capacity in the two cases, the LCD value for the horizontal position showed a 61% decrease.

From these results, it is concluded that different current ramp slopes should be used for tests at 1-g and 0-g. The values of 62 ma/min. and 7 ma/min. are reasonably close to meeting requirements, but they are not necessarily optimum. To provide for the possibility that some change in ramp slope may be

desirable as more test data is accumulated, it seems advisable that ramp slope be an adjustable parameter in the breadboard model.

Direct measurements of temperature difference between the zinc electrode surface and the body of the electrolyte in the test cell showed a temperature differential less than $1^{o}C$ under worst case conditions (1840 ma-min. discharge). It is concluded therefore that temperature gradients play an insignificant part in the convection processes present in the cell.

In preliminary tests of a Task 2 cell with a porous zinc working electrode, it has been possible to visually observe bubble distribution, and to relate this to a partial discharge capacity measurement. Current density at the electrode is an important variable in that discharge capacity difference measured with and without gas bubbles is increased with higher current density. At a current density of $\sim$100 ma/cm^2 a discharge capacity increase of $\sim$100% occurs after bubble removal. These measurements will form the basis for the Task 2 tests in which two special cells permitting direct observation and photography of Silver and Zinc electrodes respectively will be programmed to produce sequential discharge capacity measurements with gas-loaded and gas free electrodes.

Based on information received from the Yardney Electric Corporation on their HR5-DC7 Silver-Zinc battery, original test plans for Task 3 called for five 90 minute charge-discharge cycles at a discharge depth between 35 and 65% of rated capacity selected to reduce capacity by $\sim$ 1/3. Beyond 35%, Yardney expected fast attrition, while the 65% limit was set to establish charging power requirements. Initial tests of a cell of this type using the proposed test sequence were reported in the last quarterly report. These indicated a measureable loss in capacity, but less than desirable. Further tests of this type reported on here show that some samples of this type of cell show little loss in capacity within the 5 cycle test sequence even at 65%

depth of discharge. More tests of this type will be necessary to determine whether this performance is characteristic of certain individual cells only, or characteristic of this cell design.

Also evident from the results presented is the rapid rate of attrition as the number of stress cycles is increased. This suggests that a number greater than five may be a more optimum choice. Before such a change is made, however, it would be advisable to acquire similar data on more batteries of this type to insure that any decision to change the test procedure is based on a representative sample. It appears that such data could be acquired quite efficiently with the breadboard model as proposed.

SECTION IV - RECOMMENDATIONS

In the Task 1 tests, it is recommended that the current ramp rate employed under zero-g conditions be selected to give a discharged capacity approximately equivalent to that employed in Arcand's previous work at JPL. Based on results reported here a value of ~7 ma/min. appears to be required.

Success in simulating zero-g by orienting the cell electrode horizontally in order to suppress convection suggests that this orientation is the best for evaluating performance of the breadboard model. However, in order to permit correlation of test results with previous work at JPL, it is recommended that provision be made for also testing the cells in Task 1 with electrodes vertically oriented. In Task 2 tests, it is recommended that a separate electrolyte circulating system and gas separator be employed with each cell in order to insure control of evolved gases under zero-g conditions. Also recommended is the use of relatively high electrode current densities in these tests in order to accentuate the effect of gas bubble cover on electrode discharge capacity.

Based on results obtained to date in testing the Yardney HR5-DC7 battery, a considerable amount of further testing will be required in order to define an optimum test sequence for Task 3. Because of the time and expense involved in making this type of test, it is not practical to settle on a precise and rigid testing regime before construction of the Breadboard Model. A more economical approach would appear to be to use the breadboard model as an automatic testing vehicle for acquiring this type of information. In line with this philosophy, it is recommended that some additional flexibility be built into the breadboard model than was originally proposed so that more severe test regimes may be tried. This can be most readily accomplished with

the present design by increasing the maximum depth-of-discharge from 65% to 100% with the understanding that power surges may then slightly exceed the 25 watts allocated for the 2.5 volt supply.

As is evident from the data, an increase in the number of charge-discharge cycles would obviously be capable of satisfying the degradation requirements and may be desirable. Unfortunately, to do this at this stage of the breadboard model development would entail extensive changes. Since effectively the same result can be achieved with the breadboard model proposed by repeating the complete test sequence on a given cell as was done in the case of the results reported in Section 3.0, it is recommended that the breadboard model as proposed be employed to establish a precise test regime for these cells. Then, any desired changes in either the number of test cycles or depth-of-discharge can be made when the flight model of the equipment is designed.

SECTION [illegible] - NEW TECHNOLOGY

There are no "New Technology" items to be reported at this time.